Atmospheric
Chemistry
and Physics
Discussions

Open Access

Retrospective analysis of 2015-2017 winter-time PM$_{2.5}$ in China: response to emission regulations and the role of meteorology

Dan Chen[1*], Zhiquan Liu[2*], Junmei Ban[2], Pusheng Zhao[1], and Min Chen[1]

[1]Institute of Urban Meteorology, China Meteorological Administration, Beijing, 100089, China
[2]National Center for Atmospheric Research, Boulder, CO, 80301, USA

* Corresponding author: Dr. Zhiquan Liu (liuz@ucar.edu) and Dr. Dan Chen (dchen@ium.cn)

1   **Abstract**

2   To better characterize the anthropogenic emission relevant aerosol species, the GSI-WRF/Chem data

3   assimilation system was updated from the GOCART aerosol scheme to MOSAIC-4BIN scheme. Three year

4   (2015-2017) winter-time (January) surface $PM_{2.5}$ observations from 1600+ sites were assimilated hourly using

5   the updated 3DVAR system in the assimilation experiment CONC_DA. Parallel control experiment that did

6   not employ DA (NO_DA) was also performed. Both experiments were verified against the surface $PM_{2.5}$

7   observations, MODIS 550-nm AOD and also 550-nm AOD at 9 AERONET sites. In the NO_DA experiment

8   using 2010_MEIC emissions, modeled $PM_{2.5}$ are severely overestimated in Sichuan Basin (SB), Central China

9   (CC), YRD (Yangzi River Delta), and PRD (Pearl River Delta) which indicated the emissions for 2010 are not

10 appropriate for 2015-2017, as strict emission control strategies were implemented in recent years. Meanwhile,

11 underestimations in Northeastern China (NEC) and Xin Jiang (XJ) were also observed. The assimilation

12 experiments significantly reduced the high biases of surface $PM_{2.5}$ in SB, CC, YRD, and PRD, and also the

13 low biases in NEC. However the improvement of the low biases in XJ is relatively small due to the large

14 differences between the observations and the model background in the DA process, likely indicating that the

15 emissions in the model are seriously underestimated in this region. Assimilating surface $PM_{2.5}$ also

16 significantly changed the column AOD and resulted in closer agreement with MODIS data and observations

17 at AERONET sites.

18 The observations and the reanalysis data from assimilation experiment were used to investigate the year-

19 to-year changes. As the differences of the reanalysis data (CONC_DA) among years reflect combining effects

20 of meteorology and emission and the differences of modeling result from control experiment (NO_DA, with

21 same emissions) among years reflect the separate effect of meteorology, the important roles of emission and

22 meteorology in driving the changes in the three years can be distinguished and analyzed quantitatively. The

23 analysis indicated that meteorology played different roles in 2016 and 2017: the higher pressure system, lower

24 temperature and higher PBLH in 2016 are favorable for pollution dispersion (compared with 2015) while the

25 situation is almost the opposite in 2017 (compared with 2016) that leads to the increasing $PM_{2.5}$ from 2016 to

26 2017 although emission control strategies were implemented in both years. There are still large uncertainties

27 in this approach especially the inaccurate emission input in the model brings large biases in the analysis.

Atmospheric
Chemistry
and Physics
Discussions

1. Introduction

Anthropogenic $PM_{2.5}$ (fine particulate matter with aerodynamic diameters less than 2.5 µm) is known as a robust indicator of mortality and other negative health effects associated with ambient air pollution. $PM_{2.5}$ components are complicated not only from primary emissions but also from secondary formations from various precursors (e.g. SO_2, NO_x, VOCs). Regional haze with extremely high $PM_{2.5}$ concentrations (exceeding the WHO standard tenfold) has become the primary air quality concern in China, especially over the northern China (e.g. Wang *et al.* 2014a, 2014b; Han *et al.* 2015; Sun *et al.* 2015). To control the $PM_{2.5}$ pollution and improve the overall air quality, a series of strict pollution control strategies have been implemented by the government since 2010, such as *Guiding Options on Promoting the Joint Prevention and Control of Air Pollution to Improve Regional Air Quality* (The Central Government of the People's Republic of China, 2010), *Atmospheric Pollution Prevention and Control Action Plan* (The Central Government of the People's Republic of China, 2013), in which it regulated that the environmental-related equipment (Flue-gas desulfurization and Selective Catalyst Reduction, exhaust dust removal etc.) are mandatory for industries and vehicles. In addition to the long-term pollution control strategies, different emergency measures under different pollution alerts were also implemented occasionally. For example, large industrial sources (coal-burning, cement) were under limited production to reduce emission, construction sites were restricted to prevent fugitive dust pollution, traffic restrictions were implemented on even- and odd-numbered license plates etc. Those emission control strategies were even stricter and implemented more often in northern China in winter-time when the haze events occurred more frequently. These control strategies were expected to bring significant precursor (e.g. SO_2, NO_x) and $PM_{2.5}$ emission reductions.

Although with those strict emission control strategies, the ambient $PM_{2.5}$ concentrations in major cities still fluctuated in winter-time from year to year. For example, the overall January $PM_{2.5}$ concentrations in 74 cities generally decreased from 2015 to 2016, but the concentrations in January 2017 were still higher than that in 2016 (*Ambient Air Quality Monthly Report 2015-01/2016-01/2017-01*, http://www.cnemc.cn/kqzlzkbgyb2092938.jhtml). While annual emission reduction trends were expected

1   from 2015 to 2017, the overall increase of surface concentrations in January 2017 is kind of contradictory,

2   which may indicate other factors (especially meteorology) in addition to emission may play important roles.

3   Some studies attempted to investigate the variability of air pollution and also the effects of climate changes

4   on winter-time air pollution by using statistical data. Li *et al.* (2016) indicated that wintertime fog-haze days

5   across central and eastern China have close relation with East Asian Winter Monsoon; Zuo *et al.* (2015)

6   concluded that significant weakening (strengthening) Siberia high and East Asia trough are the two main key

7   factors for the extreme cold events and extreme warm events over china in winter while warm boost air

8   pollution. In addition to statistical methodology, it's necessary to distinguish the roles of emissions and

9   meteorology to further investigate the driving factors of the inter-annual air pollution changes.

10   Regional air quality models are important tools, either scientifically to understand the formation of hazes

11   or technically to make forecasts, or evaluate the effects of control strategies. For regional modeling studies,

12   emission inventory is an important part to reflect the emission input in the atmosphere. Generally, emission

13   inventory is based on the "bottom-up" methodology relying on the statistics of energy activity and emission

14   factors etc. However, uncertainties in energy statistics caused variations in the emission estimates (Zhao *et al.,*

15   2017; Hong *et al.,* 2017; Zhi *et al.*, 2017). For regional model application, the total emissions based on

16   statistics are then spatially-temporally distributed according to relevant factors (He, 2012). While the

17   occasional emission control strategies implemented in winter time caused large uncertainties in not only the

18   total emission estimation but also the spatially-temporally allocations, which would lead to large biases in the

19   model simulations.

20   In addition to the uncertainties of emission inventory, the deficiencies in chemistry also caused model

21   uncertainties. Recently, more and more observations revealed that the anthropogenic emission relevant aerosol

22   species, such as sulfate, nitrate and ammonium (denoted as SNA) are the predominant inorganic species in

23    $PM_{2.5}$ in China. Observations during the winter of 2013 (e.g. Wang *et al.*, 2014c) and autumn of 2014 (Yang

24   *et al.*, 2015) show that SNA increases rapidly during the highest haze episodes over the Northern China Plain

25   (NCP) and makes up approximately half of the total $PM_{2.5}$ mass. However, the WRF/Chem model failed to

Atmospheric
Chemistry
and Physics
Discussions

1   reproduce the highest $PM_{2.5}$ concentrations due to missing heterogeneous/aqueous reactions with either

2   GOGART (Goddard Chemistry Aerosol Radiation and Transport, Chin *et al.*, 2000, 2002) or MOSAIC (Model

3   for Simulating Aerosol Interactions and Chemistry)-4BIN aerosol schemes. In Chen *et al.* (2016, hereafter

4   Chen16), we added three heterogeneous reactions (SO_2-to-H_2SO_4 and NO_2/NO_3-to-HNO_3) in the WRF/Chem

5   model based on the MOSAIC-4BIN aerosol scheme. The new MOSAIC-4BIN aerosol scheme significantly

6   improved the simulation of sulfate, nitrate, and ammonium on polluted days in terms of both concentrations

7   and partitioning among those species.

8   Data assimilation (DA), combining observations with numerical model output, has proved to be skillful

9   at improving aerosol forecasts (e.g. Collins *et al.*, 2001; Pagowski *et al.,* 2010; Liu *et al.*, 2011; Liu *et al.,*

10   2016; Zhang *et al.,* 2016). Liu *et al.* (2011, hereafter Liu11) implemented AOD DA within the National Centers

11   for Environmental Prediction (NCEP) Gridpoint Statistical Interpolation (GSI) three-dimensional variational

12   (3DVAR) DA system coupled to the GOCART aerosol scheme within the Weather Research and

13   Forecasting/Chemistry (WRF/Chem) model (Grell *et al.*, 2005). Schwartz *et al.* (2012, hereafter S12) and

14   Jiang *et al.* (2013, hereafter Jiang13) extended the system to assimilate surface $PM_{2.5}$ and PM_{10}. Verification

15   results demonstrated improved aerosol forecasts from the DA system in studies over East Asia and also in the

16   United States.

17   Following Liu11, S12 and Chen16, we updated the GSI-WRF/Chem system: changing from the

18   GOCART aerosol scheme to MOSAIC-4BIN aerosol scheme to better characterize the complex $PM_{2.5}$

19   pollution in China. We applied the updated system to assimilate the $PM_{2.5}$ concentrations in January 2015,

20   2016 and 2017, with two purposes: 1) to reproduce the $PM_{2.5}$ trends by the DA system, and 2) to investigate

21   the different roles of meteorology and emissions for $PM_{2.5}$ pollution in different years. In this paper, section 2

22   gives model description, observations and methodology, addressing the updated GSI-WRF/Chem coupled DA

23   system with MOSAIC-4BIN aerosol scheme. In section 3, the assimilation results on $PM_{2.5}$ concentrations in

24   the January of 2015, 2016 and 2017 are presented and compared with surface observations ($PM_{2.5}$ total mass

25   and individual species) and also MODIS 550-nm AOD for evaluation of the DA system. Different from the

Atmospheric
Chemistry
and Physics
Discussions

1   previous applications emphasizing the forecast skill improvement by the DA system, we try to make full use

2   of the reanalysis data to investigate the driving factors of the pollutions, and also to separate the roles of

3   meteorology and emissions in different years by analyzing the reanalysis data and model simulations. The

4   results are given in section 4. Conclusions are given in section 5.

5   **2.   Model description, observations and methodology**

6   The WRF/Chem settings are very similar to those of Chen16, while Chen16 focused on the Sulfate-

7   Nitrate-Ammonia (SNA) aerosols in Northern China Plain during October 2014 and several heterogeneous

8   reactions were newly added to the original chemistry modules to improve the SNA simulation performance.

9   The DA system used here was based upon the NCEP GSI system extended by Liu11 and S12. We assimilated

10   surface $PM_{2.5}$ observations and the only difference is that the MOSAIC-4Bin aerosol scheme (32 species for

11   PM), instead of the GOCART aerosol scheme, was chosen in the WRF/Chem model. Thus the 3-D mass

12   mixing ratios of those MOSAIC species at each grid point comprised the analysis (or control) variables in the

13   GSI 3DVAR minimization process.

14   Here, only a brief summary of the WRF/Chem configurations follows before a description of the updated

15   GSI DA system and settings used in this work. The important differences are noted, e.g. the observation

16   forward operator in the GSI system.

17   **2.1 WRF/Chem model and emissions**

18   As in Chen16, version 3.6.1 of the WRF/Chem model was used in this study (Grell *et al.,* 2005; Fast *et*

19   *al.,* 2006). The physical parameterizations employed in WRF/Chem were identical to those of Chen16 and

20   listed in Table 1. The Carbon-Bond Mechanism version Z (CBMZ) and Model for Simulating Aerosol

21   Interactions and Chemistry (MOSAIC) were used as the gas-phase and aerosol chemical mechanisms,

22   respectively, in this study. Aerosol species in MOSAIC are defined as black carbon (BC), organic compounds

23   (OC), sulfate (SO_4), nitrate (NO_3), ammonium (NH_4), sodium (NA) and chloride (CL) and other inorganic

24   compounds (OIN). We used 4 size bins with aerosols diameters ranging from 0.039-0.1, 0.1-1.0, 1.0-2.5, and

Atmospheric
Chemistry
and Physics
Discussions

1   2.5-10 µm. The 24 variables in the first three bins (8 species times 3 bins) consist of the $PM_{2.5}$ total. The newly

2   added relative humidity (RH) dependent SO_2-to-H_2SO_4 and NO_2/NO_3-to-HNO_3 heterogeneous reactions

3   (details in Chen16) were also applied in the simulations.

4   The model domain with a 40-km horizontal grid spacing covers most of China and the surrounding region

5   (Fig. 2). There are 57 vertical levels extending from the surface to 10 hPa. The simulation started from Dec.

6   20 of previous year and the first eleven days were treated as a spin-up period and were not used in our analyses.

7   **Table 1.** WRF/Chem model configurations.

Aerosol scheme	MOSAIC (4 bins) (Zaveri *et al.*, 2008)
Photolysis scheme	Fast-J (Wild *et al.*, 2000)
Gas phase chemistry	CBM-Z (Zavier *et al.*, 1999)
Cumulus parameterization	Grell 3D scheme
Short-wave radiation	Goddard Space Flight Center Shortwave radiation scheme (Chou and Suarez, 1994)
Long-wave radiation	RRTM (Mlawer *et al.*, 1997)
Microphysics	Single-Moment 6-class scheme (Grell and Devenyi, 2002)
Land-surface model	NOAH LSM (Chen and Dudhia, 2001)
Boundary layer scheme	YSU (Hong *et al.*, 2006)
Meteorology initial and boundary conditions	GFS analysis and forecast every 6 hour
Initial condition for chemical species	11-day spin-up
Boundary conditions for chemical species	averages of mid-latitude aircraft profiles (McKeen *et al.*, 2002)
Dust and sea salt Emissions	GOCART

8   As in Chen16, the Multi-resolution Emission Inventory for China (MEIC) (Zhang *et al.*, 2009; Lei *et al.*,

9   2011; He 2012; Li *et al.*, 2014) for January 2010 is used as the emission input. The original grid spacing of

10   this emission inventory is 0.25^{o} × 0.25^{o} and it has been processed to match the model grid spacing (40 km).

11   The spatial distributions of primary $PM_{2.5}$ emission are shown in Fig. 1. The MEIC-2010 emission inventory

12   has already been applied in other studies (e.g. Wang *et al.*, 2014a; Zheng *et al.*, 2015) for simulations over

13   China for recent years. They found that this inventory provides reasonable estimates of total emissions but is

14   subject to uncertainties in the spatial allocations of these emissions over small spatial scales. For our

15   simulation, uncertainties may also arise from two other aspects: the difference between the emission base year

1   (2010) and our simulation year (2015-2016-2017), and the monthly allocations. As the China government has

2   implemented strict control strategies to insure the air quality during winter seasons since 2013, significant

3   emission reductions including the primary PM and precursor (SO_2, NO_x) in those strictly implemented regions

4   compared to the year 2010 are expected for our simulation periods. Besides, the uncertainties of the emission

5   allocation in the winter season would be much larger compared to other seasons. For example, Zhi *et al.* (2017)

6   conducted village energy survey and revealed a huge amount of missing rural raw coal for winter heating in

7   northern China which implies an extreme underestimation of rural household coal consumptions by the China

8   Energy Statistical Yearbooks.

9   **2.2 Updated GSI 3DVAR DA system**

10   NCEP's GSI 3DVAR DA system was used to assimilate surface $PM_{2.5}$ observations. The GSI 3DVAR

11   DA system calculates a best-fit "analysis" considering the observations (hourly surface $PM_{2.5}$ concentrations

12   in our case) and background fields (a 1-hr short-term WRF/Chem forecast in our case) weighted by their error

13   characteristics. The GSI 3DVAR DA system produces an analysis in model grid space. The analysis is obtained

14   through the minimization of a scalar objective function J(x) given by

15
$$J(\mathbf{x}) = \frac{1}{2}(\mathbf{x} - \mathbf{x}_b)^T \mathbf{B}^{-1}(\mathbf{x} - \mathbf{x}_b) + \frac{1}{2}[H(\mathbf{x}) - \mathbf{y}]^T \mathbf{R}^{-1}[H(\mathbf{x}) - \mathbf{y}], \qquad (1)$$

16   where $\mathbf{x_b}$ denotes the background vector (dimension m), $\mathbf{y}$ is a vector of observations (dimension p), $\mathbf{B}$ and

17   $\mathbf{R}$ represent the background and observation error covariance matrices of dimensions $m \times m$ and $p \times p$

18   respectively. The covariance matrices determine the relative contributions of the background and observation

19   terms to the final analysis. H is the potentially nonlinear "observation operator" that interpolates the model

20   grid point values to observation spaces and converts model-predicted variables to observed quantities.

21   **2.2.1 PM$_{2.5}$ observation operator**

22   In our updated DA system, GSI was used to assimilate surface $PM_{2.5}$ total mass observations. While

23   WRF/Chem model predicts $PM_{2.5}$ total mass in the forms of different prognostic variables depending on the

24   chosen aerosol scheme. As we chose the MOSAIC-4Bin aerosol schemes, the analysis variables here were the

Atmospheric
Chemistry
and Physics
Discussions

1   3D mass mixing ratios of the 24 MOSAIC aerosol variables at each grid point. Model simulated $PM_{2.5}$

2   observations $\prod m$ were computed by summing the 24 species, given as

$$\prod m = \rho_d \sum_{i=1}^{3} [BC_i + OC_i + SO_{4_i} + NO_{3_i} + NH_{4_i} + CL_i + NA_i + OIN_i]$$,   (2)

4   where i denotes the Bin numbers in the MOSAIC aerosol scheme, here the first three bins consist of the $PM_{2.5}$

5   total; BC, OC, SO_4, NO_3, NH_4, NA, CL, and OIN are black carbon, organic compounds, sulfate, nitrate,

6   ammonium, sodium, chloride and other inorganic compounds respectively. This formula is identical to the one

7   used in WRF/Chem MOSAIC scheme to diagnose $PM_{2.5}$. WRF-Chem simulated aerosol mixing ratios of the

8   species (inside the brackets of Eq. 2) are in $\mu g\, kg^{-1}$, so dry air density ρ_d is multiplied to convert the unit

9   to $\mu g\, m^{-3}$ for consistency with the observations.

10   This speciated approach to aerosol DA within a variational system was introduced by Liu11 and further

11   applied by S12 and Jiang13. By using individual aerosol species as control variables, no assumptions were

12   made regarding the contribution of each species' mass to the total aerosol mass or shapes of the vertical profiles.

13   **2.2.2 PM2.5 observations and errors**

14   Hourly surface $PM_{2.5}$ observations for January 2015-2017 were obtained from the China National

15   Environmental Monitoring Center (CNEMC). There are 1600+ sites in our modeling domain. As the 1600+

16   monitoring sites fall into 531 model grids, the observations within the same grid are averaged (the latitude

17   and longitude too) for the purpose of statistics and verification. The observation sites (Fig. 3) spanned mostly

18   in the northern, central and eastern China and are relatively sparse in western China.

19   The observation error covariance matrix **R** in equation (1) contains both measurement and

20   representativeness errors. Similar to S12 and Jiang13, the measurement error ε_0 is defined as $\varepsilon_0 = 1.0 +$

21    $0.0075 \times \prod_0$, where $\prod_0$ denotes $PM_{2.5}$ observational values (unit: $\mu g\, m^{-3}$). Following S12 and Jiang13,

22   representativeness errors is calculated as

$$\varepsilon_r = \gamma \varepsilon_0 \sqrt{\frac{\Delta x}{L}},$$ (3)

24   where γ is an adjustable parameter scaling ε_0 ($\gamma = 0.5$ was used), Δx is the grid spacing (here, 40-km)

Atmospheric
Chemistry
and Physics
Discussions

1   and L is the radius of influence of an observation and was set to 2-km for urban sites, respectively. The total

2     $PM_{2.5}$ error ($\varepsilon_{PM2.5}$) is defined as

3 $$\varepsilon_{PM2.5} = \sqrt{\varepsilon_0^2 + \varepsilon_r^2}, \tag{4}$$

4   which constituted the diagonal elements in the **R** matrix. As those $PM_{2.5}$ data were provided in near-real time

5   without any data quality control. To ensure data quality before DA, $PM_{2.5}$ observational values larger than

6     $500\mu g\ m^{-3}$ were deemed unrealistic and not assimilated. And observations leading to innovations/deviations

7   (observations minus the model-simulated values determined from the first guess fields) exceeding $120\ \mu g\ m^{-3}$

8   were also omitted.

9   **2.2.3 Background error covariance**

10   As similar to Jiang13, the background error covariance (BEC) statistics for each analysis variable

11   required by the 3DVAR algorithm were computed by utilizing the "NMC method" (Parrish and Derber, 1992)

12   based upon the one-month WRF/Chem forecasts for the winter month of January 2015. No cross-correlation

13   between the different species was considered. Standard deviations and horizontal/vertical correlation length

14   scales of the background errors (separated for each aerosol species) were calculated using the method

15   described by Wu *et al.* (2002). It is important to have the phenomena-specific background error statistics to

16   allow for an appropriate adjustment of individual species. As a function of vertical model level, the domain-

17   averaged standard deviations of the background errors for 6 aerosol species (BC, OC, SO_4, NO_3, NH_4, OIN)

18   in the first three size bins are shown in Fig. 1. CL and NA are not shown here as they are relatively too small.

19   By using the MOSAIC aerosol schemes, the characteristic of different aerosol species in different size bins

20   are more appropriately described for China region in the model. As shown in Fig. 1, the standard deviations

21   of different aerosol species errors are different in the three size bins; the errors of NO_3, OIN and SO_4 are

22   relatively larger than those of other species in the three size bins; OC is also important especially in the second

23   (0.1-1.0 μm) and third (1.0-2.5 μm) size bins. A larger background error of those species allowed larger

24   adjustment of the field, which is crucial for the aerosol analyses in this study.

Atmospheric
Chemistry
and Physics
Discussions

1 **2.3 Observations for verification**

2   In addition to the surface PM$_{2.5}$ total mass observations for data assimilation, two types of observations

3 were also used for verification: (1) MODIS monthly 550-nm AOD, (2) Surface observed 550-nm AOD at

4 AErosol RObotic NETwork (AERONET) sites. The monthly MODIS data were downloaded from

5 http://ladsweb.modaps.eosdis.nasa.gov. The Terra monthly L3 dataset (daily pass time at 10:30 Local Standard

6 Time) was used. The data resolution is $1^{o} \times 1^{o}$. As the retrieval process in winter is much difficult than the

7 other seasons, there are much missing data in western and northern China. Model simulations are averaged

8 monthly at 03 UTC (11:00 Local Standard Time) for comparison. Actually it's also an attempt to see if the

9 assimilation experiment combining regional model and surface observations can generate reasonable column

10 AOD fields; if so, this approach can be used for a complement when the satellite data are not available in

11 special cases (difficult for retrieval in certain regions). The simulated 550-nm AODs at nine AERONET sites

12 are also compared to verify the aerosol DA performance. The locations of the nine AERONET sites are shown

13 as black dots in Fig. 2. The observations obtained from AERONET are interpolated to 550-nm for comparisons

14 (Eck *et al.*, 1999).

15 **2.4 Experimental design**

16   We conducted two sets of experiments (NO_DA and CONC_DA) for January of 2015, 2016 and 2017.

17 In both cases, the MEIC_2010 emission inventory was used. The NO_DA experiment initialized a new

18 WRF/Chem forecast every 6-hr starting 00 UTC, 20 December of previous year to spin up aerosol fields and

19 run through 23 UTC, 31 January. Only simulations in January were used for analysis. In the NO_DA

20 experiment, chemical/aerosol fields were simply carried over from cycle to cycle (similar to a continuous

21 aerosol forecast) while the meteorological IC/BC were updated from GFS analysis data every 6-hr to prevent

22 meteorology simulation drifting. For CONC_DA, GSI 3DVAR updated the MOSAIC aerosol variables every

23 hour starting from 00 UTC, 1 January. The background of the first cycle at 00 UTC, 1 January was from the

24 NO_DA experiment and the later ones were from the previous cycle's 1-hr forecast. In CONC_DA, the GFS

1   analysis data in 6-hr frequency were interpolated into 1-hr data and were used to update meteorological IC/BC

2   in each 1-hr cycle. In both the NO_DA and CONC_DA experiments, the newly added heterogeneous reactions

3   were all activated.

4   **2.5 The approach to distinguish the roles of meteorology and emission**

5   As introduced in section 1, the inter-annual air quality changes are strongly influenced by both emissions

6   and meteorological conditions. It's challenging to distinguish and quantify the roles of the two aspects solely

7   based on observation or modelling. In climate forcing studies (e.g. Xu *et al.* 2017), the role of

8   climate/meteorology are diagnosed by analyzing the differences between two sets of modeling simulations

9   (with the same emission inventory but different climate/meteorology conditions). As the emission input are

10   the same, the differences between the two simulations are usually attributed to the changes of

11   climate/meteorology fields. The approach to diagnose the role of emission is somewhat similar. Gao *et al.*

12   (2017) conducted WRF/Chem simulations to distinguish the roles of meteorology and emissions during the

13   2014 APEC week in NCP when strict emission control measures were applied. As the exact emission reduction

14   ratios were publicly available in BMEPB (Beijing Municipal Environmental Protection Bureau) reports for

15   this whole event period (before, during and after the APEC week), two simulations with different emission

16   scenarios (with normal and reduced emissions) but same meteorology fields were conducted. The differences

17   between the two simulations were attributed to the changes of emissions.

18   For our case, the same methodology can be used for meteorology aspect. As for NO_DA, the emission

19   input for January of the three years (2015-2017) were all from MEIC_2010 emission inventory, the only

20   differences among the three months' simulations were meteorological condition which was from the GFS 6-

21   hr analysis data. Therefore, we can assume that the differences of simulated NO_DA $PM_{2.5}$ concentrations

22   among the three months could be driven purely by the differences in meteorological conditions (as similar to

23   Xu *et al.* 2017). However, it's difficult to distinguish the role of emission by using the same approach as in

24   Gao *et al.* (2017). As temporary emission control measures were applied according to the pollution severity

25   (alarm levels) thus the emission reduction ratios were actually kept changing during the winter season and no

Atmospheric
Chemistry
and Physics
Discussions

1   exact emission reduction ratios were provided for those days. The approach by simulations with different

2   emission scenarios is just impossible when lacking the exact emission reduction ratios. Instead, we propose

3   here a method by subtracting the meteorological effects from the total effects by utilizing the reanalysis data

4   and pure model simulations. The CONC_DA result, in which hourly surface PM$_{2.5}$ observations from 531

5   lumped sites were utilized, can be treated as a reanalysis dataset that reflects the actual conditions (very close

6   to observations). Therefore the differences of assimilated CONC_DA PM$_{2.5}$ concentrations among the three

7   months actually reflect combining effects of both meteorology and emissions. As the two experiments

8   generated gridded aerosol fields, thus we can separate the effect of emission from the total combining effects

9   by subtracting the NO_DA differences form CONC_DA differences. That gives us an idea how meteorology

10   and emission play different roles in driving the changes among the three years. Table 2 illustrates this approach

11   by taking 2015 and 2016 as an example. However, there might be some uncertainties in this approach which

12   will be discussed in detail in section 4.2.

13   **Table 2.** The approach to distinguish different roles of meteorology and emission by calculation from
14   different scenarios (take 2015 and 2016 as example).

A. Assimilated total changes	CONC_DA_2016-CONC_DA_2015	Reflecting the combining effects of all the driving factors from 2015 to 2016, e.g. emission, meteorology etc.
B. Simulated changes due to meteorology differences	NO_DA_2016-NO_DA_2015	As NO_DA_2015 and NO_DA_2016 were conducted with same emission but different meteorology, thus the differences reflect the effects from meteorological differences from 2015 to 2016
C. Calculated changes due to emission differences = (A-B)	(CONC_DA_2016-CONC_DA_2015) - (NO_DA_2016-NO_DA_2015)	Mostly reflecting the effects from emission differences from 2015 to 2016

15   **3. Verification of assimilated PM$_{2.5}$**

16   This section presents results from the NO_DA and assimilation experiments outlined above. As PM$_{2.5}$

17   has significant impact on AOD, we performed verification not only against surface PM$_{2.5}$ but also against

18   MODIS and AERONET AOD data. Slightly different from S12 and Jiang13, our purpose is to reproduce the

Atmospheric
Chemistry
and Physics
Discussions

1   spatial-temporal variations of surface $PM_{2.5}$ in the reanalysis dataset, rather than to provide the IC of aerosol

2   fields for improving forecasts.

3   **3.1 Statistics of comparison with surface $PM_{2.5}$ observations**

4   Figure 3 shows the observed and modeled monthly average of surface $PM_{2.5}$ for January in 2015, 2016

5   and 2017. Eight regions were illustrated as rectangles in the figure, including NCP (North China Plain), NEC

6   (Northeastern China), EGT (Energy Golden Triangle), XJ (Xinjiang), SB (Sichuan Basin), CC (Central China),

7   YRD (Yangzi River Delta), and PRD (Pearl River Delta). Both observation and model show that the high

8   values are mostly in NCP, SB and CC. In the NO_DA case, model results are over-predicted in SB, NCP and

9   CC for all the three months while the overestimations are more severely in SB. As the NO_DA case generally

10   overestimates (underestimates) surface $PM_{2.5}$ in NCP, SB and CC (XJ) in the three years, it may indicate that

11   the 2010 EI are not appropriate for the simulations in 2015-2017 with overestimation (underestimation)

12   respectively.

13   Compared to the NO_DA case, the assimilation experiment CONC_DA well reproduces the spatial

14   distribution of surface $PM_{2.5}$ for the three months, in terms of the relatively higher values in NCP, SB and CC

15   and also some "hot spots" in NEC, which are closer to the observations. Observations also show some "hot

16   spots" in XJ especially in 2016 and 2017 which are not captured by the NO_DA cases but much improved in

17   the CONC_DA case.

18   Basic statistical measures, including bias (BIAS), standard deviation (STDV), root-mean-square error

19   (RMSE) and correlation coefficient (CORR), are applied to evaluate the experiments. Figure 4 show the time

20   series of BIAS, STDV and RMSE for all the data used in the entire domain. The statistics are conducted for

21   each 1-hr DA cycle. After quality control, the number of $PM_{2.5}$ observations used in the DA process was

22   different from time to time, normally around 500-520 but with minimal of 320-450 for occasional times. The

23   reasons for the data filtering were from two aspects, either the $PM_{2.5}$ observational values were larger than

24   500 $\mu g\ m^{-3}$, or innovations/deviations (observations minus the model-simulated values determined from the

25   first guess fields) exceeded 120 $\mu g\ m^{-3}$, while the latter occurred more in our CONC_DA experiment. From

Atmospheric
Chemistry
and Physics
Discussions

1   the time series, we can see that the bias, STDV and RMSE are greatly improved in the CONC_DA case. The

2   maximum biases are around 50 μg m^{-3} for January 2015 and around 80 μg m^{-3} for 2016 and 2017 in NO_DA,

3   which are reduced to around ± 10 μg m^{-3} in CONC_DA. The STDV and RMSE are also reduced by at least

4   50% for most of the times.

5   Figure 5 shows the spatial distribution of the error statistics (BIAS, RMSE and CORR) at each

6   observational site (with more than 2/3 valid data in the month) in January of 2015, 2016 and 2017. We start

7   from the comparison in 2015 and then address the differences in 2016 and 2017. In NO_DA for 2015, surface

8   PM$_{2.5}$ in eastern China (NCP, SB, CC, PRD and YRD) are generally overestimated by 20-60 μg m^{-3}, but it is

9   underestimated in NEC, the Energy Golden Triangle (EGT) and especially XJ. The high biases in eastern

10   China are greatly corrected in CONC_DA. However, the low biases in EGT and XJ still exist as most of the

11   observations are just filtered out in the data QC processes. That means those observations would lead to

12   innovations exceeding 120 μg m^{-3} while such large increment probably indicates the emissions there in the

13   model are severely underestimated. Consistent with the BIAS changes in CONC_DA, the RMSE and CORR

14   in eastern China and NEC are also greatly improved with RMSE reduced by at least 50% and CORR increased

15   by 0.2-0.7. Without enough good observations being assimilated, the improvements in EGT and XJ are

16   relatively smaller. For the years of 2016 and 2017, the inhomogeneous distribution of biases in NO_DA is

17   very similar to 2015 (overestimated in eastern China but underestimated in NEC, EGT and XJ). However, the

18   high biases in CC and PRD and low biases in XJ are even larger in the latter two years. Similar to the

19   comparisons between NO_DA and CONC_DA for the year 2015, improvements are generally achieved except

20   for those sites in XJ and EGT for 2016 and 2017.

21   **3.2 Comparison with MODIS AOD and AERONET AOD**

22   As the improvement in surface PM$_{2.5}$ would bring changes in the optical depth, we also compare the

23   modeled monthly 550-nm AOD with Level-3 MODIS TERRA AOD data (Fig. 6). The MODIS AOD data are

24   of 1$^{\rm o}$ $\times$ 1$^{\rm o}$ while model resolution is 40 km $\times$ 40 km, the different resolution between the two datasets may

25   bring some uncertainties in the comparison. Besides, the MODIS TERRA AOD data are missing in NEC and

1   western China due to the retrieval process, comparisons can only be conducted for eastern China. Spatially,

2   MODIS data show the high AOD values mostly in SB and CC, around 0.5-1.0. In NO_DA, the simulated

3   AOD reached 1.4-2.8 and even larger for SB and CC which are significantly higher than the MODIS AOD.

4   After assimilation, the AOD in SB and CC are significantly decreased, which are around 1.0-2.0 in the most

5   polluted regions. It's interesting to see that although CONC_DA did reproduce the high surface $PM_{2.5}$ in NCP

6   (Fig. 3), no obvious high AOD occurred there (Fig. 6c) indicating different vertical profiles of this region. The

7   relatively simple comparison here can't be used as evidence that the 550-nm AOD after assimilation is closer

8   to MODIS data, while it did show that by assimilating surface $PM_{2.5}$, the optical depth also changed greatly.

9   The simulated 550-nm AODs at nine AERONET sites (Fig. 2) are also compared with observations to

10 verify the aerosol DA performance. As the data are only available at several time slots with large fraction of

11 missing data, thus time series are not shown here. The statistics between modeled (NO_DA/CONC_DA)

12 experiments and the observations are listed in Table 3. At most of the sites (Beijing/Beijing-

13 CAMS/Xianghe/Taihu/Hong_Kong_Poly_U/Chiayi), the NO_DA and CONC_DA are all biased low, while

14 CONC_DA didn't correct the bias but did improve the correlations. At three sites in Hongkong and Taiwan

15 (Hong_Kong_Sheung/EPA-NCU/Taipei_CWB), NO_DA results are biased high and CONC_DA help to

16 correct the overestimation and also improve the correlation. Although there are no surface $PM_{2.5}$ observations

17 in the two regions, the assimilation in surrounding regions also helps due to the transport.

18 **Table 3.** AERONET sites observed and model simulated 550-nm AOD

Site	N Pairs of Data	MEAN			RMSE		CORR	
		OBS	NO_DA	CONC_DA	NO_DA	CONC_DA	NO_DA	CONC_DA
1. Beijing	511	0.300	0.174	0.166	0.216	0.235	0.833	0.903
2. Beijing-CAMS	519	0.334	0.189	0.181	0.261	0.276	0.861	0.908
3. XiangHe	481	0.365	0.202	0.170	0.270	0.302	0.841	0.870
4. Taihu	49	0.278	0.224	0.122	0.127	0.187	0.595	0.833
5. Hong_Kong_PolyU	124	0.388	0.321	0.260	0.205	0.231	0.640	0.641
6. Hong_Kong_Sheung	39	0.313	0.642	0.134	0.486	0.224	0.520	0.663
7. EPA-NCU	58	0.269	0.470	0.254	0.390	0.178	-0.001	0.127
8. Taipei_CWB	83	0.284	0.431	0.316	0.377	0.252	0.515	0.537
9. Chiayi	254	0.457	0.233	0.163	0.330	0.371	0.545	0.363

4. Trends in 2015-2017

Given reliable $PM_{2.5}$ reanalysis fields produced by assimilating the surface $PM_{2.5}$ (CONC_DA), changing trends among the three years can be analyzed not only on scattered observational sites but also for different regions. To distinct the roles of meteorology and emissions in driving the changes, analysis based on NO_DA and CONC_DA simulations are discussed. As assumed in section 2.5, meteorology-driven changes can be analyzed in the NO_DA simulations with different meteorology but the same emission inventory for different years; while the changes of the reanalysis data in different years are actually the combination of all the driving forces, including meteorology and emission. By analyzing the two sets of simulations, we attempted to distinguish the roles of meteorology and emissions in determining the changes.

4.1 Spatial distribution

The monthly-mean $PM_{2.5}$ differences for January of the three years (2015-2017) are shown in Fig. 7, in terms of surface concentrations from observational sites (Fig. 7a) and also that from assimilation experiment (Fig. 7b). Surface observations show mostly reductions from 2015 to 2016 except for a few sites in the southern parts of NCP and EGT, and also in XJ. For the changes from 2016 to 2017, surface observations show increases at almost all the sites, especially the sites in the southern part of NCP; the only exceptions are the sites along the coastline in YRD. The assimilated (CONC_DA) differences are consistent with surface observations, that the decreasing trend from 2015 to 2016 and increasing trend from 2016 to 2017 for most of the regions are reproduced. The assimilation experiment failed to reproduce the increasing trend at XJ from 2015 to 2016 as some of the highest observations were just filtered out (section 3.1) due to the large innovations in the 3Dvar process. As already shown in Fig. 3 and indicated here again, the January of 2016 is the cleanest month among the three years.

In addition to surface $PM_{2.5}$ concentrations, the spatial distribution changes of the 550-nm AOD from MODIS retrievals (Fig. 8a) and assimilation experiment (Fig. 8b) among the three years are also shown. As too much missing data in northern and western China (Fig. 6), the trends from MODIS retrievals are only available for eastern China. Yet, the MODIS 550-nm AOD changes are still overall consistent with the surface

Atmospheric
Chemistry
and Physics
Discussions

1   observations, showing decreasing trend from 2015 to 2016 and increasing trend from 2016 to 2017 for the

2   southeastern China region. The assimilation experiment generally reproduced the trends but with some

3   shifting in the spatial distributions of decrease/increase regions compared with MODIS retrievals (especially

4   for the differences between 2017 and 2016). As the MODIS retrieval is monthly average and data filtering

5   were conducted day-to-day while model results were averaged for the whole month. That may lead to the

6   mismatch of the data period being compared.

7

8   **4.2 The roles of meteorology and emission**

9   Surface $PM_{2.5}$ concentrations from both observations and assimilation experiments show decreasing trend

10   from 2015 to 2016 but increasing trend from 2016 to 2017 for most of the regions in eastern China (Fig. 7),

11   which are also confirmed by the column AOD (Fig. 8). Actually, Chinese government has implemented strict

12   emission control strategy since 2013, especially in the northern China, and the emission reductions from year

13   to year are expected since 2013. Thus only justified from the emission aspect, the ambient response from

14   2015-2017 are just contradictory. There might be two possible assumptions: the first is the emission reduction

15   target was not achieved from 2016 to 2017, and the second is other factors are playing more important roles

16   in addition to emissions.

17   The NO_DA differences between different years are shown in Fig. 7c, which reflect the effect due to

18   meteorological condition changes (section 2.5). The effect due to emission (major factor other than

19   meteorology) is given by subtracting the NO_DA differences from the CONC_DA differences (Fig. 7d). We

20   can clearly see that the meteorology played in two different directions from 2016 to 2017. It caused decrease

21   in ambient concentrations for the northern China (NCP, NEC) from 2015 to 2016 but large increase for the

22   northern and central China (CC) from 2016 to 2017. That indicates the meteorological conditions might be

23   totally different from 2016 to 2017. After considering the impact from meteorology, the emission reduction is

24   still confirmed for the two regions from 2016 to 2017. The contributions from meteorology and emission in

25   the 8 regions (Fig. 3) were calculated and listed in Table 4. It shows around 13-18 $\mu g\ m^{-3}$ $PM_{2.5}$ reduction for

Atmospheric
Chemistry
and Physics
Discussions

1   the month of January from 2015 to 2016 in northern China (NCP, NEC), but meteorology played the

2   dominating role (contributed about 12-21 µg m^{-3} PM$_{2.5}$ reduction). The change from 2016 to 2017 in NCP and

3   NEC is totally different, meteorology caused about 12-23 µg m^{-3} PM$_{2.5}$ increase and emission control measures

4   caused 3-13 µg m^{-3} PM$_{2.5}$ decrease, that the combing effects still showed PM$_{2.5}$ increase for that region. It's

5   reasonable to say that the emission reductions for the northern regions from 2016 to 2017 are indeed obtained.

6   However, the meteorology played important role which offset the emission reduction and lead to the increase

7   of surface concentrations in 2017. The same approach is applied on the column AOD as shown in Fig. 8.

8   Consistent with surface concentrations, meteorology caused decrease/increase for northern China for the

9   period 2015-2016/2016-2017 respectively. The different roles of meteorology and emissions for different

10   regions are confirmed.

11   **Table 4.** Modeled PM$_{2.5}$ ambient concentration changes for 2016-2015, 2017-2016 and 2017-2015 in 8
12   regions, and the contributions of meteorology (MET) and emission (EMIS) calculated according to Table 2.
13   Unit: µg m^{-3}.

	2016-2015			2017-2016			2017-2015		
	Total	MET	EMIS	Total	MET	EMIS	Total	MET	EMIS
NCP	-13.38	-12.52	-0.86	+9.86	+23.16	-13.31	-3.53	+10.65	-14.17
NEC	-18.06	-21.23	+3.17	+9.60	+12.61	-3.02	-8.46	-8.62	+0.16
ETR	-1.90	-3.97	+2.07	+7.20	+12.94	-5.74	+5.30	+8.97	-3.67
XJ	-3.29	+0.07	-3.35	+5.82	+0.28	+5.55	+2.54	+0.34	+2.19
SB	-22.77	+8.72	-31.49	+9.85	+4.02	+5.83	-12.92	+12.74	-25.66
CC	-15.22	+14.12	-29.34	+5.13	+20.49	-15.35	-10.09	+34.61	-44.69
YRD	-9.03	-3.03	-5.99	-11.65	-2.93	-8.73	-20.68	-5.96	-14.72
PRD	-24.07	+13.02	-37.09	+13.20	-6.12	+19.32	-10.87	+6.90	-17.78

14

15   It is worth noting that there are uncertainties in the simulation/assimilation processes. Firstly, emission

16   inventories are obviously not accurate in the NO_DA simulations which may bring uncertainty in the analysis.

17   For example, the emission in SB, CC and PRD are generally overestimated (Fig. 3), which means the ambient

18   concentration changes might be artificially amplified in considering the meteorology impacts (Fig. 7c and Fig.

19   8c). Secondly, the meteorological IC/BC conditions in NO_DA simulations, which were from GFS analysis

20   data every 6-hr, have also uncertainties. The biases in meteorological conditions might lead to uncertainties in

Atmospheric
Chemistry
and Physics
Discussions

1   the $PM_{2.5}$ analysis. Thirdly, the accuracy of the CONC_DA assimilation experiment also affects the analysis.

2   For example, the assimilation did reproduce some of the "hot spots" in XJ (Fig. 3c) but can't reproduce the

3   increasing trends from 2015 to 2016 (Fig. 7b) as some of the highest concentrations in 2016 were not well

4   simulated (Fig. 3c). Finally, the contribution of aerosol-meteorology feedback was not considered in our

5   calculation. As pointed out by Gao *et al.* (2017), reduced aerosol feedbacks due to emission reductions account

6   for about 10.9% of the total decreases in $PM_{2.5}$ concentrations in urban Beijing in their APEC study. In our

7   current approach, this effect is combined in the emission aspects in the subtracting process.

8   **4.3 Meteorology changes in 2016 and 2017**

9   It's interesting to see that meteorology played different roles in the three years. Here we compared some

10   meteorology parameters to explain the meteorology impacts. Differences of monthly mean boundary layer

11   height (PBLH), surface pressure (PSFC), 2-meter temperature (T2), 2-meter relative humidity (RH2) and 10-

12   meter wind speed in different years are given in Fig. 9. It shows that the changes of PSFC and T2 for the

13   period 2015-2016 and 2016-2017 are totally different for the whole region. Compared to 2015, the pressure

14   system is stronger, temperature is lower, and wind speed is larger in most regions in 2016 which are favorable

15   for pollution dispersion. While there are some unfavorable conditions including lower PBLH and higher RH

16   (thus more reactions) in the northern and southern China which may offset the impacts of high pressure system

17   and low temperature. So the combining impacts of those meteorological parameters caused ambient

18   concentration decrease in northern China and increase in southern China from 2015 to 2016 as shown in Fig.

19   7 and Fig. 8. For the changes from 2016 to 2017, meteorological changes are totally different with weaker

20   pressure system, higher temperature, smaller wind speed, and lower PBLH in most regions, which caused the

21   pollution accumulation. As suggested by recent studies, climate change has important impacts on extreme

22   haze events in northern China based on historical statistical approach or by using climate models. Those

23   studies (e.g. Li *et al.*, 2015, Zuo *et al.*, 2015) revealed that wintertime fog-haze days across central and eastern

24   China have close relation with East Asian Winter Monsoon; significant weakening (strengthening) Siberia

25   high and East Asia trough are the two main key factors for the extreme cold events and extreme warm events

Atmospheric
Chemistry
and Physics
Discussions

1   over china in winter; while warm boosts air pollution. Consistent with our study, Zhao *et al.* (2018) pointed

2   out that stronger Siberian High period in January 2016 produced a significant decrease in $PM_{2.5}$ concentrations

3   than that during the weaker ones in other years. Those studies emphasized climate change factors, the impacts

4   of emission changes are still difficult to evaluate. Our study used the DA technique combining regional models

5   and surface observations, aiming to separate the factors of emission and meteorology, thus to further

6   investigate the year-to-year changes for the regional scale.

7   **5. Conclusions**

8   To analyze the complex $PM_{2.5}$ pollution in China, the GSI-WRF/Chem aerosol data assimilation system

9   was updated from the GOCART aerosol scheme to MOSAIC-4BIN scheme, which is more appropriate to

10   characterize the anthropogenic emission relevant aerosol species. Three-year (2015-2017) winter-time

11   (January) surface $PM_{2.5}$ observations from 1600+ sites were assimilated hourly using the updated 3DVAR

12   system in the assimilation experiment CONC_DA. Parallel control experiment that did not employ DA

13   (NO_DA) was also performed.

14   Both the control and the assimilation experiments were verified against the surface $PM_{2.5}$ observations,

15   MODIS and AERONET 550-nm AOD. In the NO_DA experiment that 2010_MEIC emission inventory was

16   used, modeled $PM_{2.5}$ were severely overestimated in Sichuan Basin (SB), Central China (CC), YRD (Yangzi

17   River Delta), and PRD (Pearl River Delta) which indicated the emissions for 2010 are not appropriate for

18   2015-2017, as strict emission control strategies were implemented in recent years. Meanwhile,

19   underestimations in Northeastern China (NEC) and Xin Jiang (XJ) were also observed.

20   The assimilation experiment significantly reduced the high biases of surface $PM_{2.5}$ in SB, CC, YRD, and

21   PRD, and also low biases in NEC. However, the improvement of the low biases in XJ is relatively small as

22   some of the observations were filtered out in the DA system due to the large innovations which are treated as

23   "unrealistic"; those large innovations also indicate that the emissions in the model are seriously underestimated

24   in this region. Assimilating surface $PM_{2.5}$ also significantly changes the column AOD; comparisons with

Atmospheric
Chemistry
and Physics
Discussions

1   MODIS 550-nm AOD showed that the control experiment without DA are too high in eastern China and that

2   of assimilation experiment are more close to MODIS data.

3   Both observation and assimilation experiment showed decreasing ambient concentration from 2015 to

4   2016 but increasing from 2016 to 2017 for most of the regions. To distinct the important roles driving the

5   changes, the reanalysis data from assimilation experiment and modeling result from control experiment were

6   analyzed. It shows around 13-18 $\mu g\, m^{-3}$ $PM_{2.5}$ reduction for the month of January from 2015 to 2016 in northern

7   China (NCP, NEC), but meteorology played the dominating role (contributed about 12-21 $\mu g\, m^{-3}$ $PM_{2.5}$

8   reduction). The change from 2016 to 2017 in NCP and NEC is totally different, meteorology caused about 12-

9   23 $\mu g\, m^{-3}$ $PM_{2.5}$ increase and emission control measures caused 3-13 $\mu g\, m^{-3}$ $PM_{2.5}$ decrease, that the combing

10   effects still showed $PM_{2.5}$ increase for that region. The analysis approved that meteorology played different

11   roles in 2016 and 2017: the higher pressure system, lower temperature and higher PBLH in 2016 are favorable

12   for pollution dispersion (compared with 2015); the situation is almost the opposite in 2017 (compared with

13   2016) that leads to the increasing $PM_{2.5}$ from 2016 to 2017, although emission control strategy were

14   implemented in both years. After considering the impacts from meteorology, the analysis showed that the

15   emission reductions were indeed obtained from 2015 to 2016 and 2017, especially in NCP for the year 2017

16   (although surface concentrations were increasing that year).

17   While there are still large uncertainties in this approach, as the inaccurate emission input, uncertainties

18   in the meteorological IC/BC and assimilation process, and also the imperfection of aerosol-meteorology

19   feedbacks in the model simulation bring large biases in the analysis. The most straightforward way is to

20   directly estimate the emissions by data assimilation, which will be the topic in a separate study.

Atmospheric
Chemistry
and Physics
Discussions

References

Chen, D., Liu, Z. Q., Fast, J., and Ban, J. M.: Simulations of sulfate-nitrate-ammonium (SNA) aerosols during the extreme haze events over northern China in October 2014, Atmos. Chem. Phys., 16, 10707-10724, 10.5194/acp-16-10707-2016, 2016.

Chen, F., and Dudhia, J.: Coupling an advanced land surface-hydrology model with the Penn State-NCAR MM5 modeling system. Part I: Model implementation and sensitivity, Mon. Weather Rev., 129, 569-585, 2001.

China National Environmental Monitoring Center, Ambient Air Quality Monthly Report 2015-01/2016-01/2017-01; http://www.cnemc.cn/kqzlzkbgyb2092938.jhtml.

Chin, M., Savoie, D. L., Huebert, B. J., Bandy, A. R., Thornton, D. C., Bates, T. S., Quinn, P. K., Saltzman, E. S., and De Bruyn, W. J.: Atmospheric sulfur cycle simulated in the global model GOCART: Comparison with field observations and regional budgets, J. Geophys. Res.-Atmos., 105, 24689-24712, doi:10.1029/2000jd900385, 2000.

Chin, M., Ginoux, P., Kinne, S., Torres, O., Holben, B. N., Duncan, B. N., Martin, R. V., Logan, J. A., Higurashi, A., and Nakajima, T.: Tropospheric aerosol optical thickness from the GOCART model and comparisons with satellite and Sun photometer measurements, J. Atmos. Sci., 59, 461-483, doi:10.1175/1520-0469(2002)059<0461:Taotft>2.0.Co;2, 2002.

Chou, M.-D., and M.J. Suarez.: An efficient thermal infrared radiation parameterization for use in general circulation models, NASA Tech. Memo., TM 104606, vol. 3, 25 pp., NASA Goddard Space Flight Cent., Greenbelt, Md. 1994

Collins, W. D., Rasch, P. J., Eaton, B. E., Khattatov, B. V., Lamarque, J. F., and Zender, C. S.: Simulating aerosols using a chemical transport model with assimilation of satellite aerosol retrievals: Methodology for INDOEX, J. Geophys. Res.-Atmos., 106, 7313-7336, doi:10.1029/2000jd900507, 2001.

Fast, J. D., Gustafson, W. I., Easter, R. C., Zaveri, R. A., Barnard, J. C., Chapman, E. G., Grell, G. A., and Peckham, S. E.: Evolution of ozone, particulates, and aerosol direct radiative forcing in the vicinity of Houston using a fully coupled meteorology-chemistry-aerosol model, J. Geophys. Res.-Atmos., 111, D21305, doi:10.1029/2005jd006721, 2006.

Gao, M., Liu, Z., Wang, Y., Lu, X., Ji, D., Wang, L., Li, M., Wang, Z., Zhang, Q., Carmichael., G. R.: Distinguishing the roles of meteorology, emission control measures, regional transport, and co-benefits of reduced aerosol feedbacks in "APEC Blue". Atmos. Environ., 167, 476-486, doi:10.1016/j.atmosenv.2017.08.054, 2017.

Grell, G. A., Peckham, S. E., Schmitz, R., McKeen, S. A., Frost, G., Skamarock, W. C., and Eder, B.: Fully coupled "online" chemistry within the WRF model, Atmos. Environ., 39, 6957-6975, doi:10.1016/j.atmosenv.2005.04.027, 2005.

Grell, G. A., and Devenyi, D.: A generalized approach to parameterizing convection combining ensemble and data assimilation techniques, Geophys. Res. Lett., 29, Artn 1693.Doi 10.1029/2002gl015311, 2002.

Han, B., Zhang, R., Yang, W., Bai, Z., Ma, Z., and Zhang, W.: Heavy air pollution episodes in Beijing during January 2013: inorganic ion chemistry and source analysis using Highly Time-Resolved Measurements in an urban site, Atmos. Chem. Phys. Discuss., 15, 11111-11141, doi:10.5194/acpd-15-11111-2015, 2015.

He, K.B., Multi-resolution emission Inventory for China (MEIC): model framework and 1990-2010 anthropogenic emissions. In: Presented on the international Global Atmospheric Chemistry Conference, September 17-21, Beijing, China 2012

Hong, C. P., Zhang, Q., He, K. B., Guan, D. B., Li, M., Liu, F., and Zheng, B.: Variations of China's emission estimates: response to uncertainties in energy statistics, Atmos. Chem. Phys., 17, 1227-1239, 10.5194/acp-17-1227-2017, 2017.

Atmospheric
Chemistry
and Physics
Discussions

Hong, S. Y., Noh, Y., and Dudhia, J.: A new vertical diffusion package with an explicit treatment of entrainment processes, Mon. Weather Rev., 134, 2318-2341, 2006.

Jiang, Z., Z. Liu, T. Wang, C. S. Schwartz, H.-C. Lin, and F. Jiang.: Probing into the impact of 3DVAR assimilation of surface PM10 observations over China using process analysis, J. Geophys. Res. Atmos., 118, 6738–6749, doi:10.1002/jgrd.50495, 2013.

Liu, J., Han, Y., Tang, X., Zhu, J., Zhu, T.: Estimating adult mortality attributable to PM2.5 exposure in China with assimilated PM2.5 concentrations based on a ground monitoring network. Sci. Total Environ., 568, 1253-1262, 2016.

Liu, Z. Q., Liu, Q. H., Lin, H. C., Schwartz, C. S., Lee, Y. H., and Wang, T. J.: Three-dimensional variational assimilation of MODIS aerosol optical depth: Implementation and application to a dust storm over East Asia, J. Geophys. Res.-Atmos., 116, Artn D23206. doi:10.1029/2011jd016159, 2011.

Lei, Y., Zhang, Q., He, K. B., and Streets, D. G.: Primary anthropogenic aerosol emission trends for China, 1990-2005, Atmos. Chem. Phys., 11, 931-954, 10.5194/acp-11-931-2011, 2011.

Li, M., Zhang, Q., Streets, D. G., He, K. B., Cheng, Y. F., Emmons, L. K., Huo, H., Kang, S. C., Lu, Z., Shao, M., Su, H., Yu, X., and Zhang, Y.: Mapping Asian anthropogenic emissions of non-methane volatile organic compounds to multiple chemical mechanisms, Atmos. Chem. Phys., 14, 5617-5638, 10.5194/acp-14-5617-2014, 2014.

Li, Q., Zhang, R. H., and Wang, Y.: Interannual variation of the wintertime fog-haze days across central and eastern China and its relation with East Asian winter monsoon, Int. J. Climatol., 36, 346-354, 10.1002/joc.4350, 2016.

McKeen, S. A., Wotawa, G., Parrish, D. D., Holloway, J. S., Buhr, M. P., Hubler, G., Fehsenfeld, F. C., and Meagher, J. F.: Ozone production from Canadian wildfires during June and July of 1995, J. Geophys. Res.-Atmos., 107, 4192, doi:10.1029/2001jd000697, 2002.

Mlawer, E. J., Taubman, S. J., Brown, P. D., Iacono, M. J., and Clough, S. A.: Radiative transfer for inhomogeneous atmospheres: RRTM, a validated correlated-k model for the longwave, J. Geophys. Res.-Atmos., 102, 16663-16682, 1997.

Pagowski, M., Grell, G. A., McKeen, S. A., Peckham, S. E., and Devenyi D.: Three dimensional variational data assimilation of ozone and fine particulate matter observations: some results using the Weather Research and Forecasting-Chemistry model and Grid-point Statistical Interpolation, Q. J. R. Meteorol. Soc., 136(653), 2010.

Sun, Y. L., Wang, Z. F., Du, W., Zhang, Q., Wang, Q. Q., Fu, P. Q., Pan, X. L., Li, J., Jayne, J., and Worsnop, D. R.: Long-term real-time measurements of aerosol particle composition in Beijing, China: seasonal variations, meteorological effects, and source analysis, Atmos. Chem. Phys., 15, 10149-10165, 10.5194/acp-15-10149-2015, 2015.

Schwartz, C. S., Z. Liu, H. C. Lin, and S. A. McKeen.: Simultaneous three-dimensional variational assimilation of surface fine particulate matter and MODIS aerosol optical depth, J. Geophys. Res.-Atmos., 117, 2012.

The Central People's Government of the People Republic of China. Guiding Opinions on Promoting the Joint Prevention and Control of Air Pollution to Improve Regional Air Quality, Beijing. 2010.

The Central People's Government of the People Republic of China. Atmospheric Pollution Prevention and Control Action Plan. 2013.

Wang, L. T., Wei, Z., Yang, J., Zhang, Y., Zhang, F. F., Su, J., Meng, C. C., and Zhang, Q.: The 2013 severe haze over southern Hebei, China: model evaluation, source apportionment, and policy implications, Atmos. Chem. Phys., 14, 3151-3173, 10.5194/acp-14-3151-2014, 2014a.

Atmospheric
Chemistry
and Physics
Discussions

Wang, W., Maenhaut, W., Yang, W., Liu, X. D., Bai, Z. P., Zhang, T., Claeys, M., Cachier, H., Dong, S. P., and Wang, Y. L.: One-year aerosol characterization study for $PM_{2.5}$ and PM10 in Beijing, Atmos. Pollut. Res., 5, 554-562, 10.5094/Apr.2014.064, 2014b.

Wang, Y. S., Yao, L., Wang, L. L., Liu, Z. R., Ji, D. S., Tang, G. Q., Zhang, J. K., Sun, Y., Hu, B., and Xin, J. Y.: Mechanism for the formation of the January 2013 heavy haze pollution episode over central and eastern China, Sci. China Earth Sci., 57, 14-25, 10.1007/s11430-013-4773-4, 2014c.

Wild, O., Zhu, X., and Prather, M. J.: Fast-j: Accurate simulation of in- and below-cloud photolysis in tropospheric chemical models, J. Atmos. Chem., 37, 245-282, 2000.

Xu, J., Chang, L., Yan, F., and He, J.: Role of climate anomalies on decadal variation in the occurrence of wintertime haze in the Yangtze River Delta, China. Science of the Total Environment,599-600, 918-925, doi:10.1016/j.scitotenv.2017.05.015, 2017.

Yang, Y. R., Liu, X. G., Qu, Y., An, J. L., Jiang, R., Zhang, Y. H., Sun, Y. L., Wu, Z. J., Zhang, F., Xu, W. Q., and Ma, Q. X.: Characteristics and formation mechanism of continuous hazes in China: a case study during the autumn of 2014 in the North China Plain, Atmos. Chem. Phys., 15, 8165-8178, 10.5194/acp-15-8165-2015, 2015.

Zhang, L., Shao, J., Lu, X., Zhao, Y., Hu, Y., Henze, D. K., Liao, H., Gong, S., Zhang, Q.: Sources and Processes Affecting Fine Particulate Matter Pollution over North China: An Adjoint Analysis of the Beijing APEC Period. Environ. Sci. Technol., 50, 8731-8740, 2016.

Zhang, Q., Streets, D. G., Carmichael, G. R., He, K. B., Huo, H., Kannari, A., Klimont, Z., Park, I. S., Reddy, S., Fu, J. S., Chen, D., Duan, L., Lei, Y., Wang, L. T., and Yao, Z. L.: Asian emissions in 2006 for the NASA INTEX-B mission, Atmos. Chem. Phys., 9, 5131-5153, 2009.

Zaveri, R. A., and Peters, L. K.: A new lumped structure photochemical mechanism for large-scale applications, J. Geophys. Res.-Atmos., 104, 30387-30415, 1999.

Zaveri, R. A., Easter, R. C., Fast, J. D., and Peters, L. K.: Model for Simulating Aerosol Interactions and Chemistry (MOSAIC), J. Geophys. Res.-Atmos., 113, D13204, doi:10.1029/2007jd008782, 2008.

Zhao, S., Feng, T., Tie, X., Long, X., Li, G., Cao, J., Zhou, W., and An, Z.: Impact of Climate Change on Siberian High and Wintertime Air Pollution in China in Past Two Decades, Earth's Future, 6, 118–133, https://doi.org/10.1002/2017EF000682, 2018.

Zhao, Y., Zhou, Y. D., Qiu, L. P., and Zhang, J.: Quantifying the uncertainties of China's emission inventory for industrial sources: From national to provincial and city scales, Atmos. Environ., 165, 207-221, 10.1016/j.atmosenv.2017.06.045, 2017.

Zheng, B., Zhang, Q., Zhang, Y., He, K. B., Wang, K., Zheng, G. J., Duan, F. K., Ma, Y. L., and Kimoto, T.: Heterogeneous chemistry: a mechanism missing in current models to explain secondary inorganic aerosol formation during the January 2013 haze episode in North China, Atmos. Chem. Phys., 15, 2031-2049, 10.5194/acp-15-2031-2015, 2015.

Zhi, G. R., Zhang, Y. Y., Sun, J. Z., Cheng, M. M., Dang, H. Y., Liu, S. J., Yang, J. C., Zhang, Y. Z., Xue, Z. G., Li, S. Y., and Meng, F.: Village energy survey reveals missing rural raw coal in northern China: Significance in science and policy, Environ. Pollut., 223, 705-712, 10.1016/j.envpol.2017.02.009, 2017.

Zuo, Z. Y., Zhang, R. H., Huang, Y., Xiao, D., and Guo, D.: Extreme cold and warm events over China in wintertime, Int. J. Climatol., 35, 3568-3581, 10.1002/joc.4229, 2015.

Atmospheric
Chemistry
and Physics
Discussions

1   **Tables and Figures**

2   **Table 1.** WRF/Chem model configurations.

3   **Table 2.** The approach to distinguish different roles of meteorology and emission by calculation from different
4   scenarios (take 2015 and 2016 as example).

5   **Table 3.** AERONET sites observed and model simulated 550-nm AOD.

6   **Table 4.** Modeled $PM_{2.5}$ ambient concentration changes for 2016-2015, 2017-2016 and 2017-2015 in 8 regions
7   and the contributions of meteorology (MET) and emission (EMIS) calculated according to Table 2. Unit: µg
8   m^{-3}.

9   **Figure 1.** Domain-averaged standard deviations of background errors (µg kg^{-1}) as a function of height for
10 each aerosol variables in three bins: (a) Bin-01 0.039-0.1 µm, (b) Bin-02 0.1-1.0 µm, (c) Bin-03 1.0-2.5 µm.

11 **Figure 2.** Spatial distribution of $PM_{2.5}$ emissions (unit: µg m^{-2} s^{-1}) used in this study. Black dots with numbers
12 indicate 9 AErosol RObotic NETwork (AERONET) sites used for aerosol optical depth verification: 1-Beijing
13 (39.98ºN, 116.38ºE), 2-Beijing-CAMS (39.93ºN, 116.32ºE), 3-XiangHe (39.75ºN, 116.96ºE), 4-Taihu
14 (31.42ºN, 120.22ºE), 5-Hong_Kong_PolyU (22.30ºN, 114.18ºE), 6-Hong_kong_Sheung (22.48ºN,
15 114.117ºE), 7-EPA-NCU (24.97ºN, 121.19ºE), 8-Taipei_CWB (25.03ºN, 121.50ºE), 9-Chiayi (23.50ºN,
16 120.50ºE).

17 **Figure 3.** Observed and modeled monthly average of $PM_{2.5}$ concentrations (unit: µg m^{-3}) for January in 2015
18 (Left), 2016 (middle) and 2017 (right). Regions defined in red rectangles are: a-NCP (North China Plain), b-
19 NEC (Northeastern China), c- EGT (Energy Golden Triangle), d-XJ (Xinjiang), e-SB (Sichuan Basin), f-CC
20 (Central China), g-YRD (Yangzi River Delta), h-PRD (Pearl River Delta).

21 **Figure 4.** The time series of statistics between model simulations and observations. Red lines- CONC_DA
22 minus observation, blue lines –NO_DA minus observation. Statistics include number of data pairs, MEAN-
23 mean bias, STDV- standard deviation, RMS-root mean square error. Left-2015, middle-2016, right-2017.
24 (Unit are µg m^{-3} for MEAN, STDV and RMS).

25 **Figure 5.** The spatial distribution of statistics between model simulations and observations for January, (a)
26 2015, (b) 2016, (c) 2017. Top: NO_DA v.s. observation, bottom: CONC_DA v.s. observation. BIAS-model
27 minus observation, RMSE-root mean square error, CORR-correlation coefficient. (Unit is µg m^{-3} for BIAS
28 and RMSE).

29 **Figure 6.** Observed and modeled monthly average of 550-nm AOD for January in 2015 (Left), 2016 (middle)
30 and 2017 (right). Observation (a) is from MODIS Terra monthly L3 dataset (daily path time at 10:30 Local
31 Standard Time). Model simulations from (b) NO_DA and (c) CONC_DA are monthly averages at 03 UTC
32 (11:00 Local Standard Time). (d) The difference of CONC_DA minus NO_DA.

33 **Figure 7.** Observed and modeled $PM_{2.5}$ ambient concentration changes for 2016-2015 (left), 2017-2016
34 (middle) and 2017-2015 (right). (a) Observations, (b) Assimilated total changes, (c) Modeled changed due to
35 meteorology conditions, (d) Calculated changes due to emission. (Unit: µg m^{-3})

36 **Figure 8.** Similar to Figure 7 but for observed and modeled 550-nm AOD changes.

37 **Figure 9.** Modeled meteorological changes for 2016-2015 (left), 2017-2016 (middle) and 2017-2015 (right).
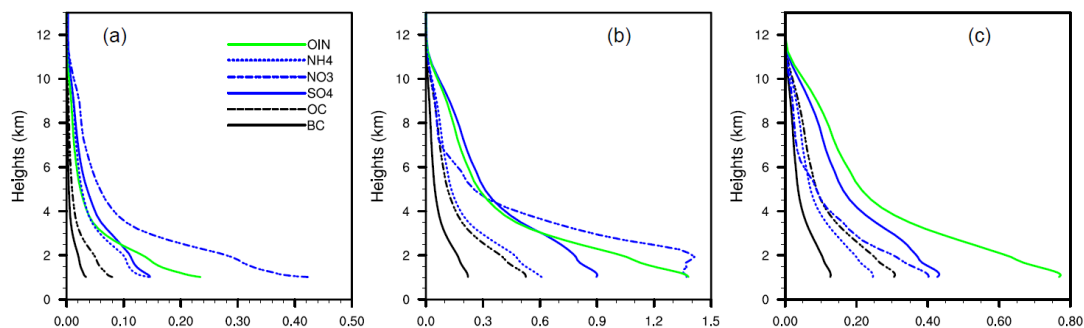38 (a) PBLH, (b) PSFC, (c) T2, (d) RH2 and (e) 10-m wind speed.

Atmospheric
Chemistry
and Physics
Discussions

Figure 1. Domain-averaged standard deviations of background errors (µg kg^{-1}) as a function of height for each aerosol variables in three bins: (a) Bin-01 0.039-0.1 µm, (b) Bin-02 0.1-1.0 µm, (c) Bin-03 1.0-2.5 µm.
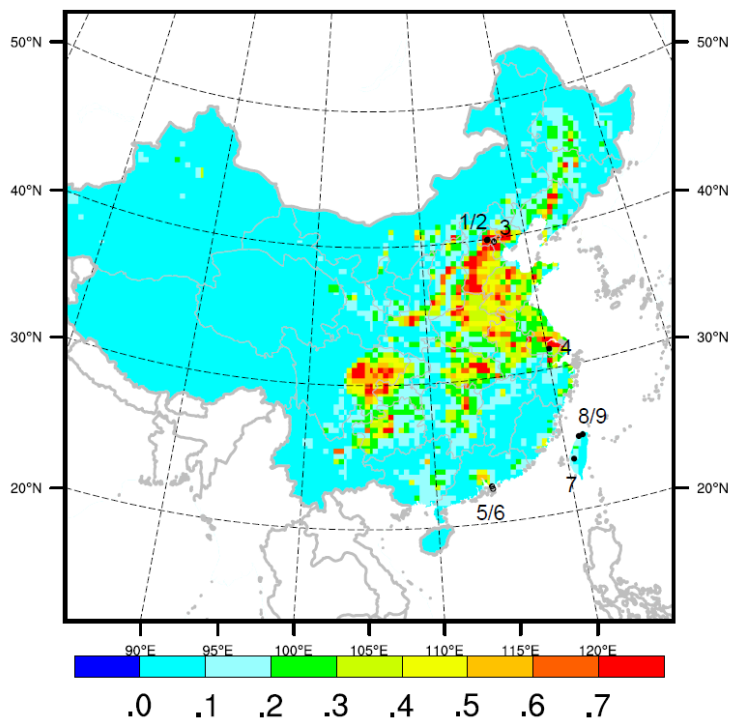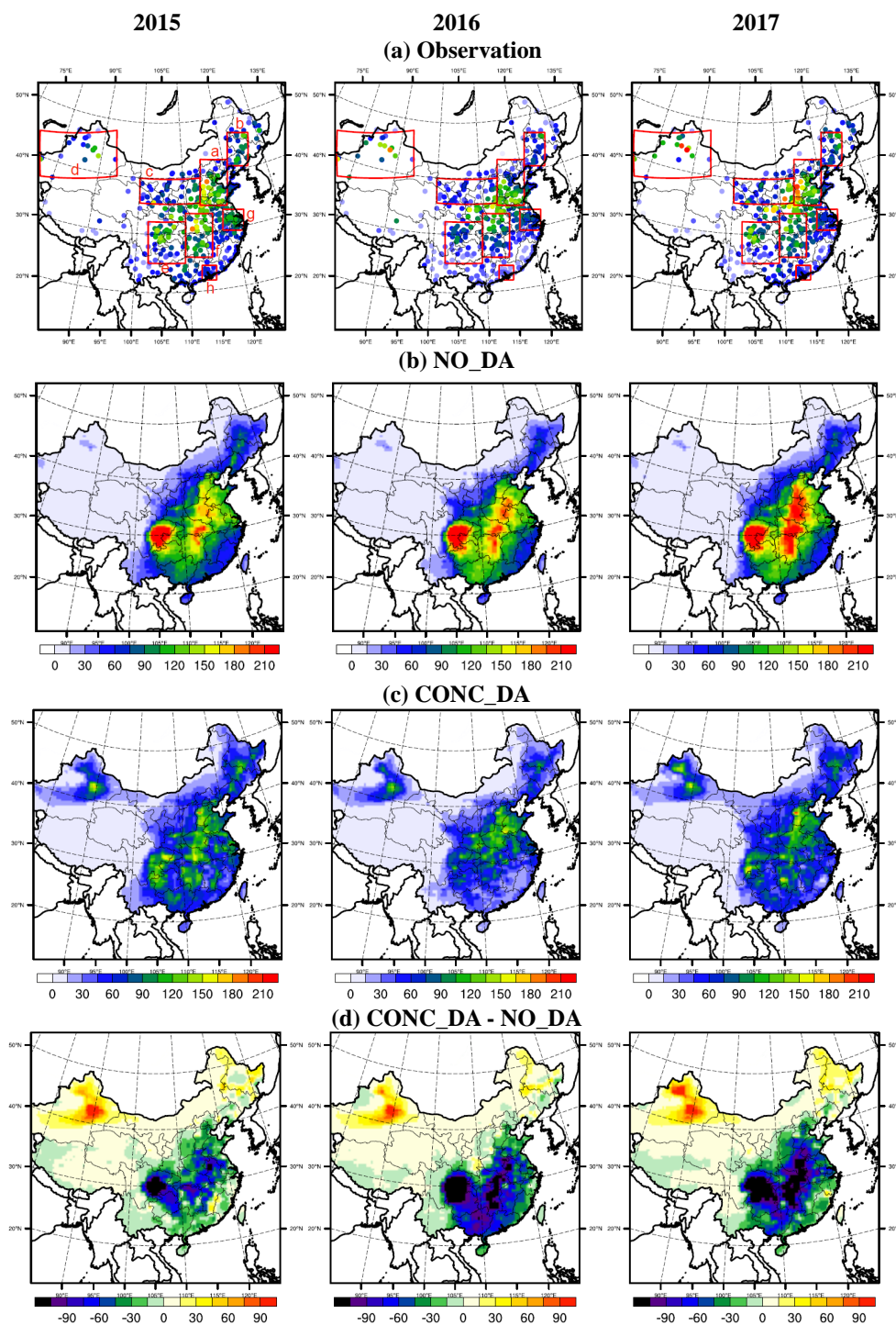
Atmospheric
Chemistry
and Physics
Discussions

Figure 2. Spatial distribution of PM$_{2.5}$ emissions (unit: µg m^{-2} s^{-1}) used in this study. Black dots with numbers indicate 9 AErosol RObotic NETwork (AERONET) sites used for aerosol optical depth verification: 1-Beijing (39.98^{o} N, 116.38^{o} E), 2-Beijing-CAMS (39.93^{o} N, 116.32^{o} E), 3-XiangHe (39.75^{o} N, 116.96^{o} E), 4-Taihu (31.42^{o} N, 120.22^{o} E), 5-Hong_Kong_PolyU (22.30^{o} N, 114.18^{o} E), 6-Hong_kong_Sheung (22.48^{o} N, 114.117 ^{o} E), 7-EPA-NCU (24.97^{o} N, 121.19^{o} E), 8-Taipei_CWB (25.03^{o} N, 121.50^{o} E), 9-Chiayi (23.50^{o} N, 120.50^{o} E).

Figure 3. Observed and modeled monthly average of PM$_{2.5}$ concentrations (unit: µg m^{-3}) for January in 2015 (Left), 2016 (middle) and 2017 (right). Regions defined in red rectangles are: a-NCP (North China Plain), b-NEC (Northeastern China), c- EGT (Energy Golden Triangle), d-XJ (Xinjiang), e-SB (Sichuan Basin), f-CC (Central China), g-YRD (Yangzi River Delta), h-PRD (Pearl River Delta).
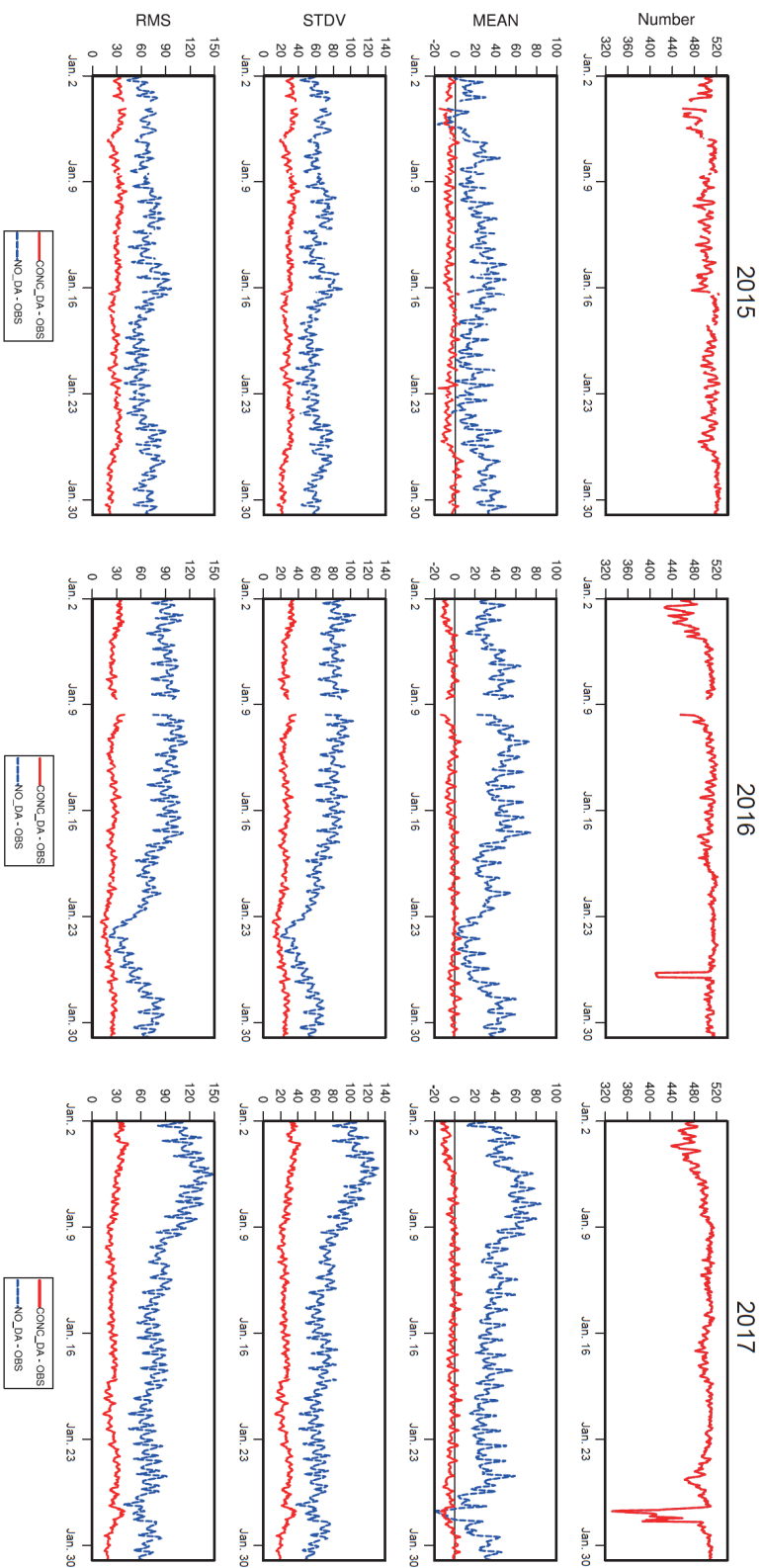
Figure 4. The time series of statistics between model simulations and observations. Red lines- CONC_DA minus observation, blue lines –NO_DA minus observation. Statistics include number of data pairs, MEAN-mean bias, STDV- standard deviation, RMSE-root mean square error. Left-2015, middle-2016, right-2017. (Unit are μg m⁻³ for MEAN, STDV and RMS).

(a). 2015 - NO_DA (top) and CONC_DA (bottom)
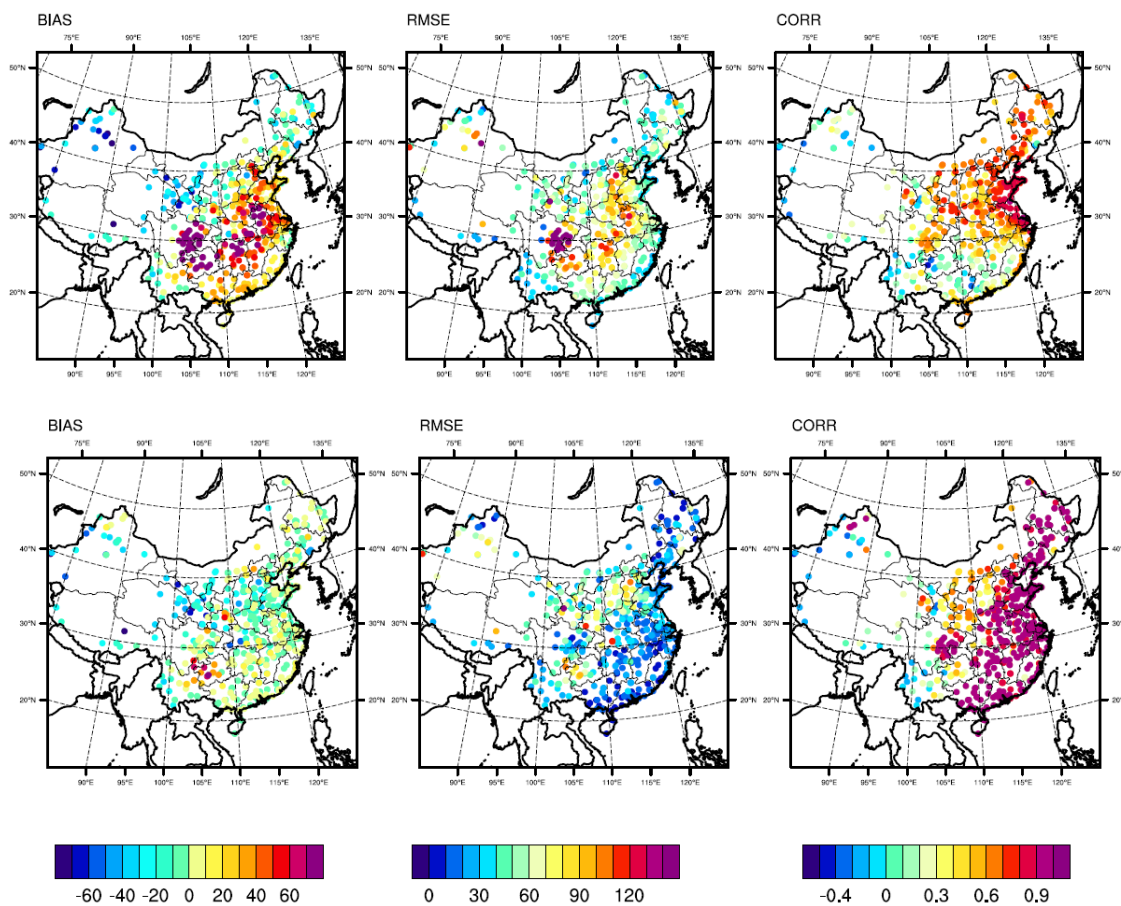
Figure 5a. The spatial distribution of statistics between model simulations and observations for January 2015. Top: NO_DA v.s. observation, bottom: CONC_DA v.s. observation. BIAS-model minus observation, RMSE-root mean square error, CORR-correlation coefficient. (Unit is µg m^{-3} for BIAS and RMSE).
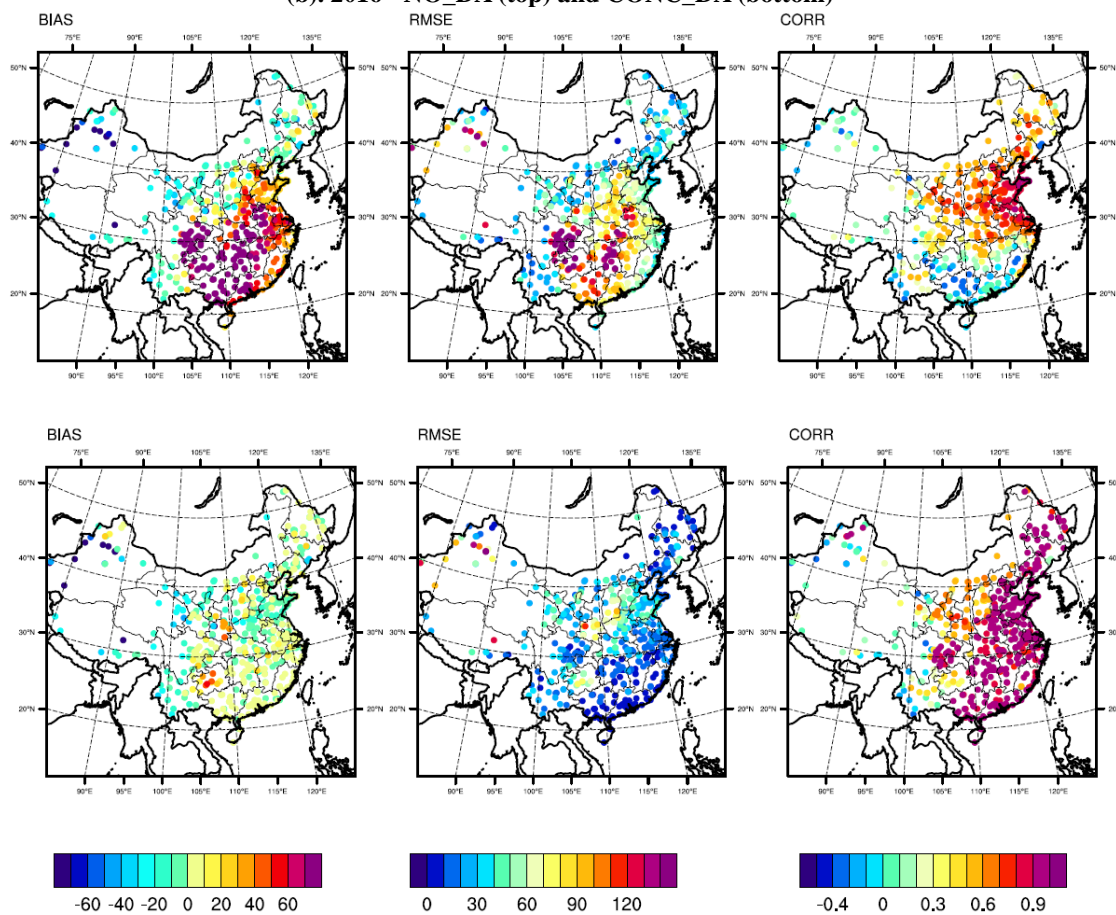
Figure 5b. Continue. Same as Figure 5a but for 2016.

Atmospheric
Chemistry
and Physics
Discussions

(c). 2017 - NO_DA (top) and CONC_DA (bottom)
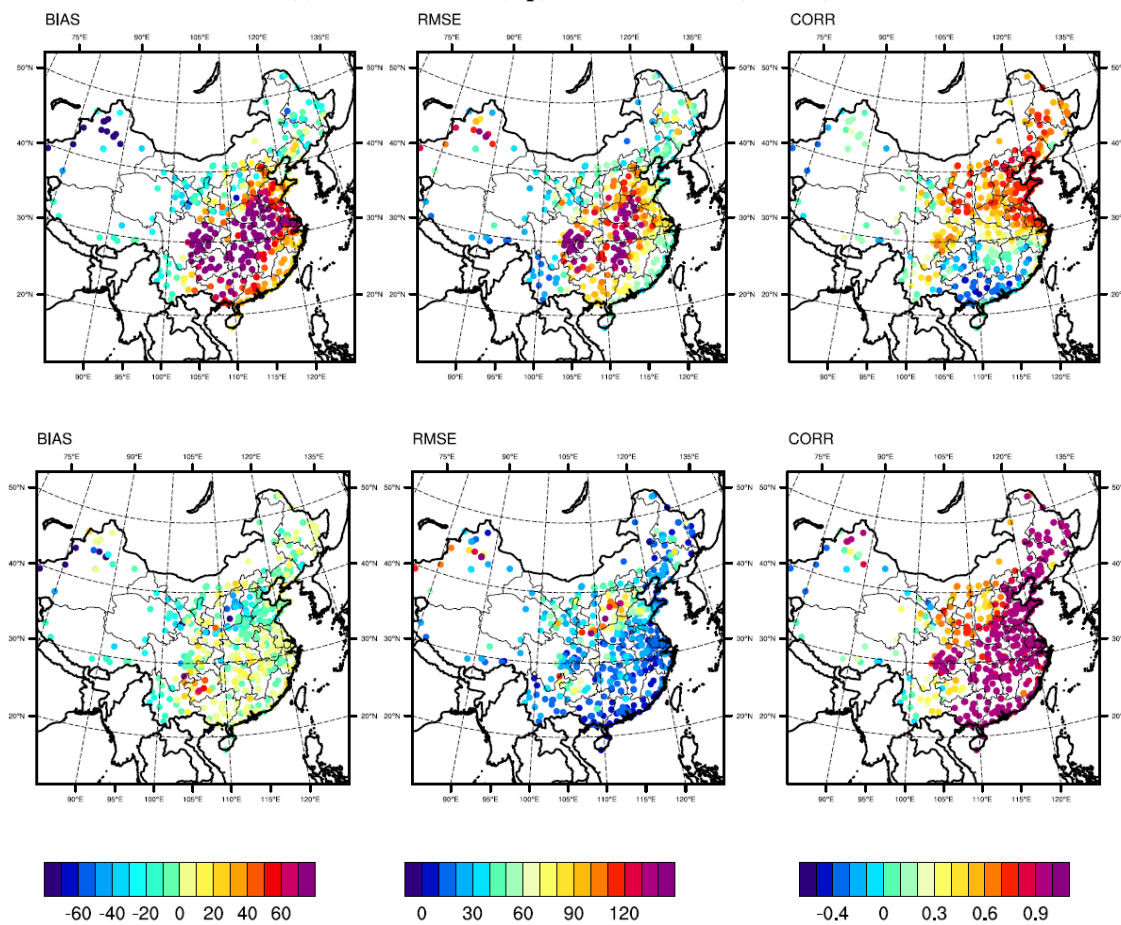
Figure 5c. Continue. Same as Figure 5a but for 2017.
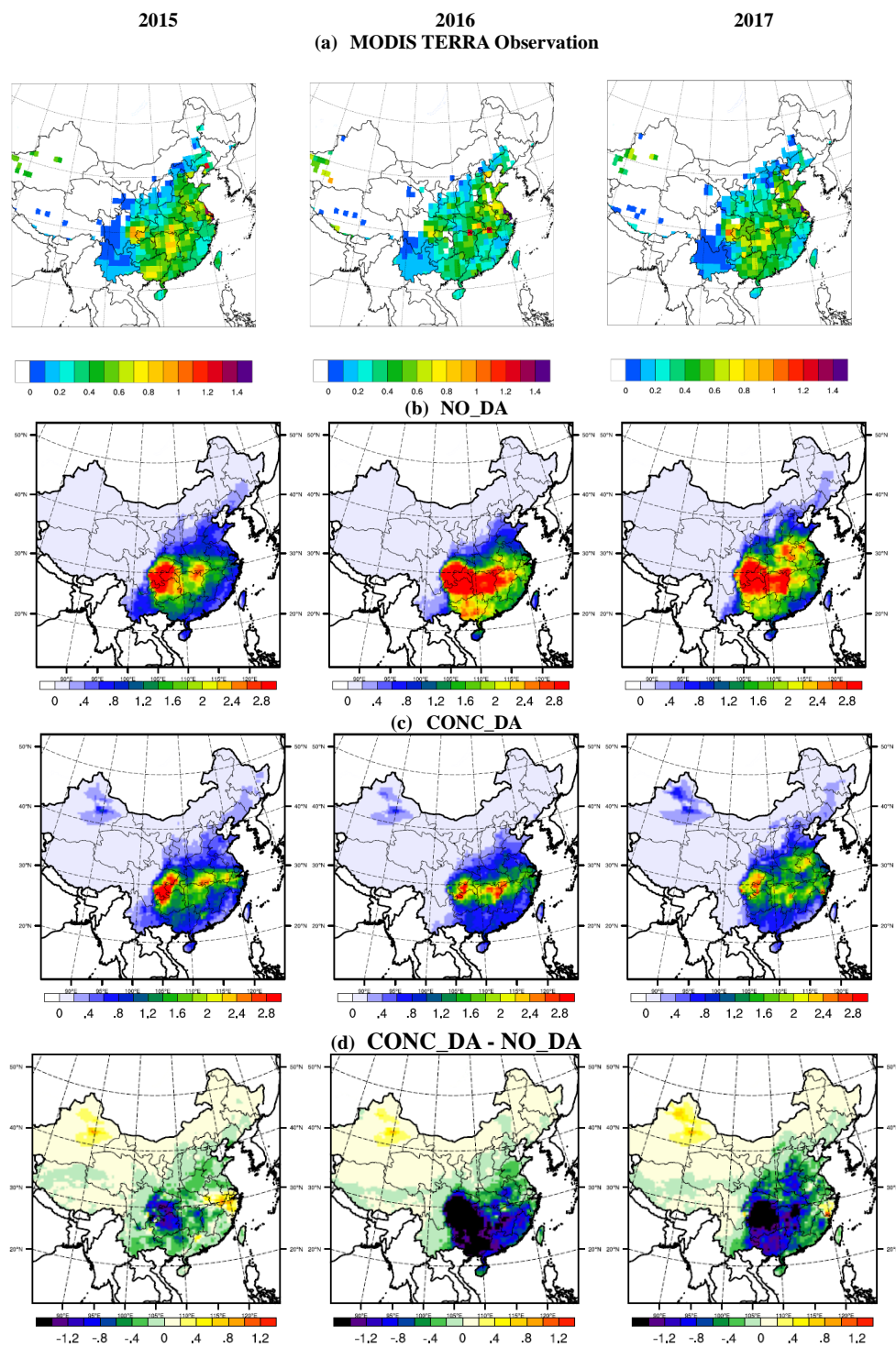
Atmospheric
Chemistry
and Physics
Discussions

Figure 6. Observed and modeled monthly average of 550-nm AOD for January in 2015 (Left), 2016 (middle) and 2017 (right). Observation (a) is from MODIS Terra monthly L3 dataset (daily path time at 10:30 Local Standard Time). Model simulations from (b) NO_DA and (c) CONC_DA are monthly averages at 03 UTC (11:00 Local Standard Time). (d) The difference of CONC_DA minus NO_DA.
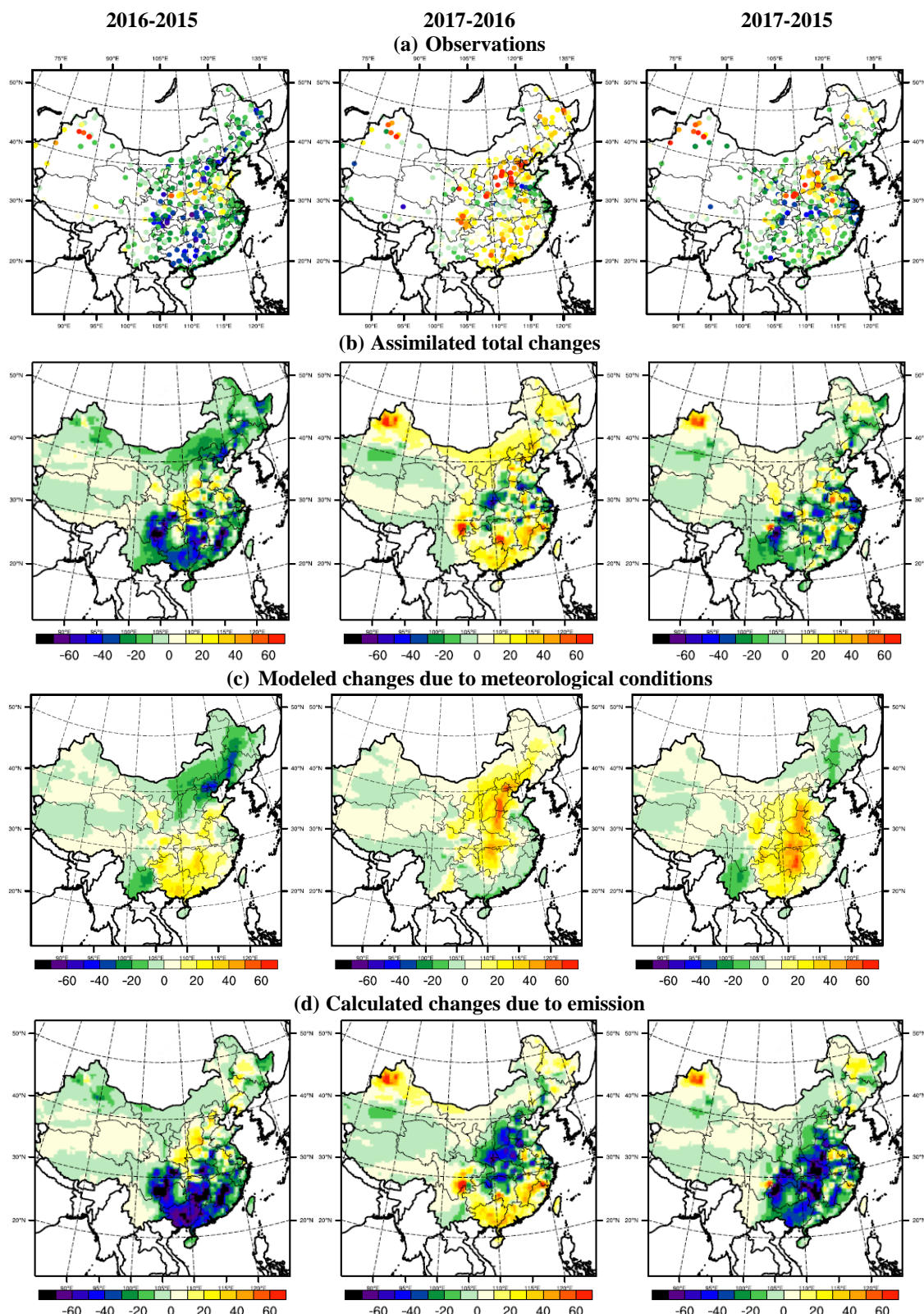
Atmospheric
Chemistry
and Physics
Discussions

Figure 7. Observed and modeled PM$_{2.5}$ ambient concentration changes for 2016-2015 (left), 2017-2016 (middle) and 2017-2015 (right). (Unit: μg m^{-3}).
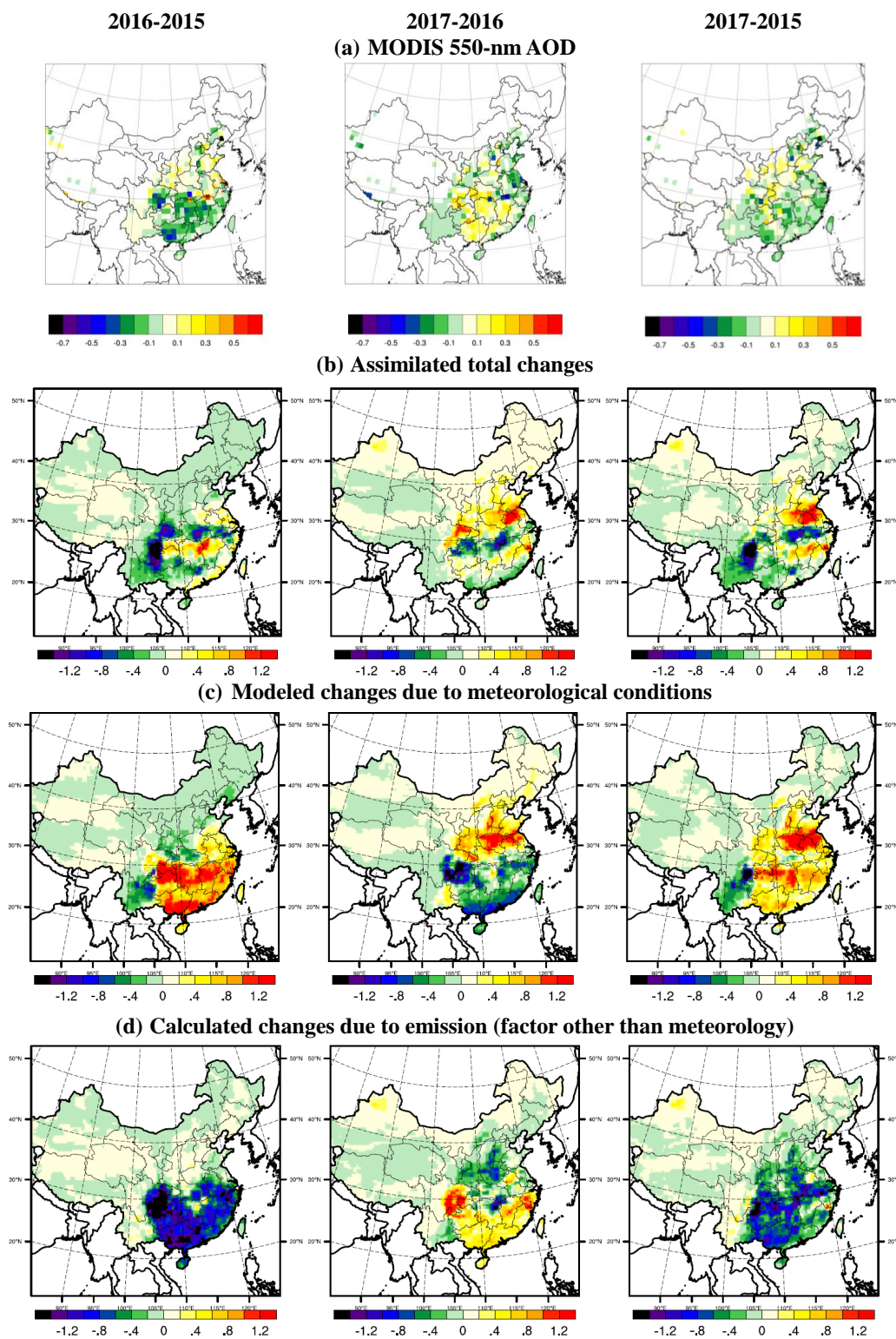
Figure 8. Similar to Figure 7 but for observed and modeled 550-nm AOD changes.
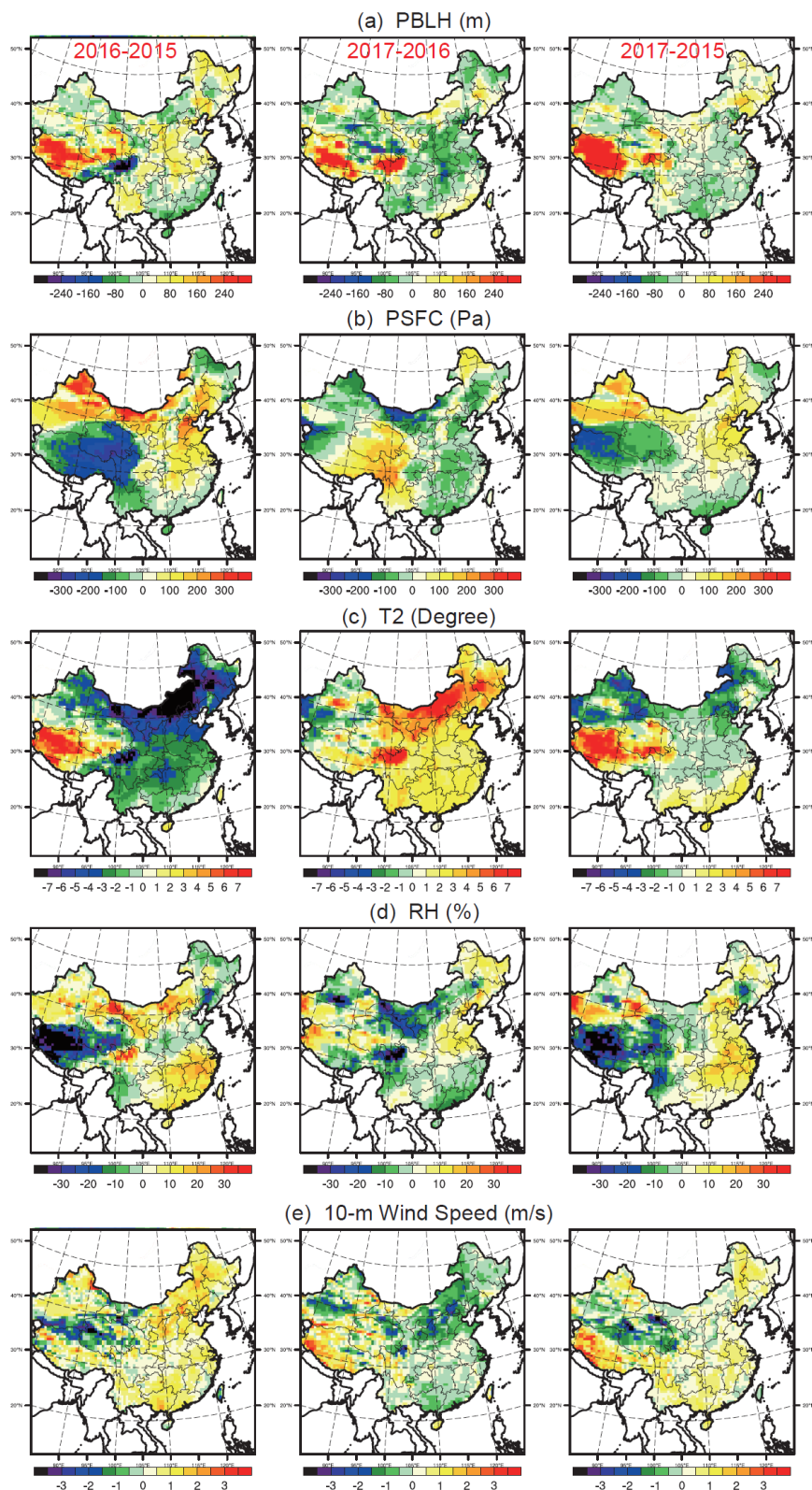
Figure 9. Modeled meteorological changes for 2016-2015 (left), 2017-2016 (middle) and 2017-2015 (right) for (a) PBLH, (b) PSFC, (c) T2, (d) RH2 and (e) 10-m wind speed.